Neuroscience

Cholinergic input to mouse visual cortex signals a movement state and acutely enhances layer 5 responsiveness

Baba Yogesh, Georg B. Keller

Friedrich Miescher Institute for Biomedical Research, Basel, Switzerland • Faculty of Natural Sciences, University of Basel, Basel, Switzerland

Reviewed Preprint

Revised by authors after peer review.

About eLife's process

Reviewed preprint version 2
February 13, 2024 (this version)

Reviewed preprint version 1
September 25, 2023

Sent for peer review
June 28, 2023

Posted to preprint server
June 12, 2023

Abstract

Acetylcholine is released in visual cortex by axonal projections from the basal forebrain. The signals conveyed by these projections and their computational significance are still unclear. Using two-photon calcium imaging in behaving mice, we show that basal forebrain cholinergic axons in the mouse visual cortex provide a binary locomotion state signal. In these axons, we found no evidence of responses to visual stimuli or visuomotor prediction errors. While optogenetic activation of cholinergic axons in visual cortex in isolation did not drive local neuronal activity, when paired with visuomotor stimuli, it resulted in layer-specific increases of neuronal activity. Responses in layer 5 neurons to both top-down and bottom-up inputs were increased in amplitude and decreased in latency, whereas those in layer 2/3 neurons remained unchanged. Using opto- and chemogenetic manipulations of cholinergic activity, we found acetylcholine to underlie the locomotion-associated decorrelation of activity between neurons in both layer 2/3 and layer 5. Our results suggest that acetylcholine augments the responsiveness of layer 5 neurons to inputs from outside of the local network, enabling faster switching between internal representations during locomotion.

eLife assessment

This **important** study by Yogesh and Keller provides a set of results describing the response properties of cholinergic input and its functional impacts in the mouse visual cortex. They found that cholinergic inputs are elevated by locomotion in a binary manner regardless of locomotor speeds, and activation of cholinergic input differently modulated the activity of Later 2/3 and Layer 5 visual cortex neurons induced by bottom-up (visual stimuli) and top-down (visuomotor mismatch) inputs. The reviewers found that the experiments are cutting-edge and well executed, and the results to be mostly **convincing**.

Introduction

Acetylcholine is one of the key neuromodulators involved in cortical function and plasticity. A rich body of work has shown that acetylcholine gates experience-dependent changes in the responses of cortical neurons to sensory inputs. This includes receptive field plasticity in auditory cortex (Bakin et al., 2012; Froemke et al., 2007; Kilgard and Merzenich, 1998; Metherate and Weinberger, 1990), somatosensory cortex (Ego-Stengel et al., 2001; Rasmusson and Dykes, 1988; Sachdev et al., 1998), and olfactory cortex (Wilson et al., 2004), or ocular dominance plasticity in visual cortex (Bear and Singer, 1986; Greuel et al., 1988; Gu and Singer, 1993; Kirkwood et al., 1999). In all cases, the central tenet is that pairing of acetylcholine release or its application concurrent with a sensory stimulus results in plasticity that increases the responsiveness of neurons to subsequent presentations of the same stimulus. While the evidence that acetylcholine gates plasticity is overwhelming and unequivocal, it remains less well understood what drives the release of acetylcholine in cortex during behavior and what its functional consequences are on cortical computations acutely.

Cholinergic projections to cortex arise from a population of neurons in the basal forebrain (Li et al., 2018). Within this population of neurons, there is a relatively broad functional heterogeneity (Laszlovszky et al., 2020; Robert et al., 2021), with responses observed during movement – be it locomotion or licking (Harrison et al., 2016), to reinforcers (Hangya et al., 2015), to auditory stimuli (Guo et al., 2019; Robert et al., 2021), and weakly to visual stimuli (Robert et al., 2021). However, inferring acetylcholine release in specific cortical targets based on activity of cholinergic neurons within the basal forebrain is complicated by the fact that different regions (Kim et al., 2016; Pinto et al., 2013) and cholinergic cell types (Laszlovszky et al., 2020) in the basal forebrain project to different areas of cortex. This projection specificity likely underlies the heterogeneity in cholinergic activity across dorsal cortex (Collins et al., 2023; Lohani et al., 2022). Measurements of cholinergic activity in cortex have found that movement in the form of a lever press is associated with cholinergic activity in mouse motor cortex, somatosensory cortex, and prefrontal cortex (Ren et al., 2022). Whisking is associated with cholinergic axonal activity in barrel cortex (Eggermann et al., 2014), while sound (Zhu et al., 2023) and movement (Nelson and Mooney, 2016; Zhu et al., 2023) are associated with cholinergic activity in auditory cortex, and locomotion (Larsen et al., 2018; Lohani et al., 2022), facial movement (Lohani et al., 2022), and pupil dilation (Larsen et al., 2018; Reimer et al., 2016) are associated with cholinergic activity in visual cortex. Overall, cholinergic activity in cortex is closely related to movement, but whether movement is the primary determinant of cholinergic activity and how movement related activity compares to sensory driven activity is less clear.

Likely the primary functional effect of increased levels of acetylcholine in cortex is increased sensory responsiveness. Local application of acetylcholine has been shown to increase sensory responses in somatosensory cortex (Chatfield and Dempsey, 1941), auditory cortex (Forster and McCarter, 1946), as well as visual cortex (Sato et al., 1987) in anesthetized cats. A similar gain in visually evoked responses in rodent visual cortex can be induced by iontophoretic application of acetylcholine in cortex (Sillito and Kemp, 1983), by systemic acetylcholine release following basal forebrain stimulation (Goard and Dan, 2009; Pafundo et al., 2016), or by optogenetic stimulation of basal forebrain cholinergic axons in visual cortex (Pinto et al., 2013). Interestingly, this increase of sensory responses caused by acetylcholine is not homogeneous across cortical layers. Neurons responsive to iontophoretic application of acetylcholine are preferentially found in deep cortical layers (Krnjević and Phillis, 1963). The effects of acetylcholine are primarily one of facilitation of neuronal responses in deep cortical layers and one of suppression in superficial layers (Sillito and Kemp, 1983; Soma et al., 2013). However, depending on how locally acetylcholine is applied, it can also result in selective hyperpolarization of layer 5 neurons (Gulledge et al., 2007). Triggering systemic increase of acetylcholine by nucleus basalis stimulation results in firing rate increases in layers 4, 5, and 6 of visual cortex, but decreased firing rates in layer 2/3 (Goard and Dan, 2009). While it is unclear whether the effect

observed in the experiments that use systemic modulation of cholinergic activity is cortical or reflects a combination of changes in subcortical and cortical processing, a direct layer-specific effect on cortical processing would be consistent with differential expression of acetylcholine receptors across cortical layers (Obermayer et al., 2017). Based on these findings it is often assumed that the local release of acetylcholine in cortex differentially influences deep and superficial cortical layers.

A second functional effect of acetylcholine is a decorrelation of cortical activity. Both basal forebrain cholinergic neuron stimulation and local cholinergic axon stimulation in visual cortex desynchronizes activity in visual cortex (Pinto et al., 2013). This effect is thought to be mediated by the influence of acetylcholine on somatostatin positive interneurons and their interaction with the excitatory neurons. This is based on the finding that optogenetic inhibition of somatostatin interneurons blocks acetylcholine induced decorrelation (Chen et al., 2015), and that optogenetically induced acetylcholine release selectively enhances the input from excitatory neurons onto somatostatin interneurons (Urban-Ciecko et al., 2018). A similar decrease in correlation has also been observed during locomotion (Aydın et al., 2018; Erisken et al., 2014), and the effect was stronger in deeper layers of cortex (Dadarlat and Stryker, 2017). It is possible that the decrease of correlations observed during locomotion is driven by locomotion related increases in acetylcholine.

More generally, following the discovery of the modulation of sensory evoked responses by locomotion in visual cortex (Niell and Stryker, 2010), it has been speculated that acetylcholine is involved in locomotion related changes in neuronal activity. Based on studies in rodents, a circuit was delineated that projects from mesencephalic locomotor region to the basal forebrain, which when active, can bring about a gain of responses in visual cortex to visual stimuli (Lee et al., 2014). It has been argued that nicotinic activation of vasoactive intestinal peptide (VIP) expressing interneurons in visual cortex is necessary for this locomotion induced gain of visual responses (Fu et al., 2014). While VIP interneurons are clearly influenced by acetylcholine (Gasselin et al., 2021), cholinergic receptors are expressed in all cortical cell types (Colangelo et al., 2019), and there are likely direct functional effects of acetylcholine on many other cell types (Alitto and Dan, 2012; Chen et al., 2015; Gulledge and Stuart, 2005; Hay et al., 2016; Hedrick and Waters, 2015; Unal et al., 2012; Xiang, 1998; Zolles et al., 2009). This has called into question the interpretation that acetylcholine is involved in locomotion related changes in neuronal activity primarily through nicotinic activation of VIP neurons (Pakan et al., 2016). The specific subtypes of muscarinic and nicotinic receptors expressed across these different cell types further complicate causal attribution of effects. Nevertheless, all these lines of evidence come together to suggest that basal forebrain cholinergic axons in visual cortex increase their activity on locomotion and release acetylcholine to bring about a gain of visually evoked responses. However, a direct measurement of the activity of cholinergic projection from basal forebrain to visual cortex during locomotion has not been made. Throughout the manuscript, we will refer to basal forebrain cholinergic axons simply as cholinergic axons. This distinction notably excludes potential axons that arise from local VIP-ChAT^{+} neurons (Granger et al., 2020), that are labeled when using a cross of ChAT-Cre mice with a reporter line. Prior measurements of the activity of cholinergic axons in visual cortex have all relied on data from a cross of ChAT-Cre mice with a reporter line (Larsen et al., 2018; Reimer et al., 2016).

In this work, we sought to understand the signals conveyed by the basal forebrain cholinergic system to visual cortex, the consequent changes to activity of layer 2/3 and layer 5 neurons in visual cortex upon release of acetylcholine, and the potential implications this could have on the computations performed by visual cortex. We used two-photon calcium imaging of cholinergic axons in visual cortex in behaving head-fixed mice and found that cholinergic activity in visual cortex was best approximated as a locomotion state signal. The effects of optogenetic activation of

cholinergic axons locally in visual cortex were layer-specific: the responsiveness was increased in neurons in layer 5 but not in layer 2/3. Furthermore, we provide evidence that acetylcholine release underlies the locomotion related decorrelation of activity in visual cortex.

Results

To investigate the function of cholinergic input to visual cortex, we first characterized the calcium activity in these axons. We used an AAV vector to express an axon-targeted GCaMP6s (Broussard et al., 2018) in basal forebrain cholinergic neurons using ChAT-IRES-Cre mice (Rossi et al., 2011) and recorded calcium activity of their axons in visual cortex using two-photon microscopy (**Figures 1A and 1B**). For imaging experiments, mice were head-fixed on a spherical treadmill surrounded by a toroidal screen (**Figure 1C**). We used a set of different visuomotor conditions known to activate neurons in visual cortex to probe for activation of cholinergic axons. First, mice were exposed to a closed loop condition during which locomotion velocity was coupled to movement in a virtual tunnel. We then measured activity in an open loop condition during which locomotion and movement in the virtual tunnel were uncoupled, in darkness, and during presentation of full field drifting gratings. Throughout all experimental conditions mice were free to locomote on the spherical treadmill.

We found that the activity in many cholinergic axons strongly increased during locomotion (**Figures 1D and 1E**). Activity increased with locomotion onset (**Figure 1F**) with an average lag across all responsive axons of 477 ms relative to locomotion onset (**Figure S1A**). Thus, consistent with results reported for auditory cortex (Nelson and Mooney, 2016), we found that locomotion preceded the increase in cholinergic activity in visual cortex. Locomotion onset also results in an increase in activity of neurons in primary visual cortex (Ayaz et al., 2013; Keller et al., 2012; Saleem et al., 2013). It has been speculated that cholinergic input is a driver of locomotion related activity in visual cortex (Lee et al., 2014). We thus compared the observed response latency between cholinergic input and activity of layer 2/3 and layer 5 neurons. The response latency of cholinergic axons was longer than the latency we observed in responses of layer 2/3 neurons (**Figure S1B**), but shorter than that of layer 5 neurons (**Figures S1C and S1D**). This would suggest that the initial increase in neuronal activity in layer 2/3 of the visual cortex was not driven by cholinergic input from basal forebrain.

Interestingly, we found no evidence of a response of cholinergic axons to other stimuli that drive responses in visual cortex such as full field drifting gratings (**Figure 1G**), visual flow onsets in open loop (**Figure 1H**), or visuomotor mismatches (**Figure 1I**) (Attinger et al., 2017; Jordan and Keller, 2020; Keller et al., 2012; Niell and Stryker, 2008; Vasilevskaya et al., 2023; Widmer et al., 2022). Visuomotor mismatches are brief visual flow halts that break the coupling between locomotion and visual flow feedback in a closed loop condition. Consistent with the absence of response to visual stimuli – full field drifting gratings or visual flow in open loop, we found that the response to locomotion onset was independent of whether the locomotion occurred in darkness, in the presence of visual stimuli, or with visual flow feedback coupled to locomotion (**Figure 1J**). For each imaging site, we then quantified the percentage of cholinergic axons that exhibited significant responses to locomotion onset, full field drifting gratings, or visuomotor mismatch, and found that 52.3% ± 4.4% (mean ± SEM) of the axons responded significantly to locomotion onset, while the fraction of responsive axons to gratings and mismatch was not different from chance (**Figure 1K**).

To confirm that an increase in calcium activity in cholinergic axons corresponds to an increase in extracellular acetylcholine, we measured acetylcholine levels using the genetically-encoded acetylcholine sensor GRAB-Ach3.0 (Jing et al., 2020). The sensor was expressed in visual cortex, and we performed two-photon imaging in layer 2/3 during the same visuomotor conditions as described above. We found that consistent with the calcium activity of cholinergic axons,

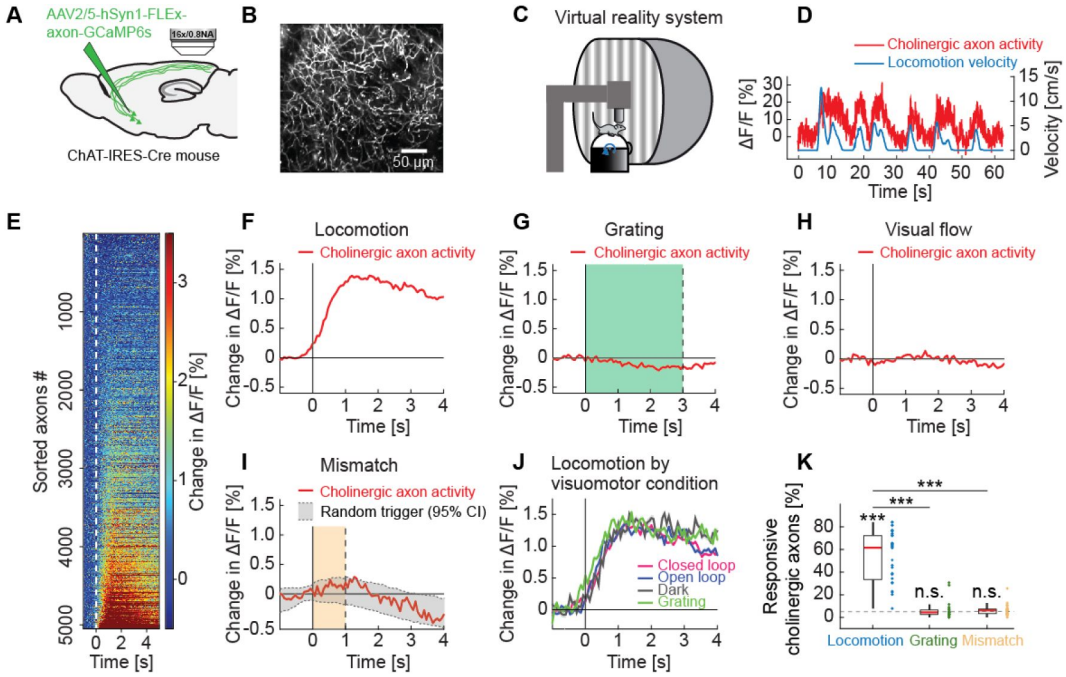

Figure 1.

Cholinergic axons in visual cortex are activated during locomotion independent of visual stimuli.

(**A**) GCaMP6s was expressed by injecting an AAV2/5-hSyn1-FLEx-axon-GCaMP6s vector in basal forebrain of ChAT-IRES-Cre mice. We then imaged calcium activity of cholinergic axons projecting to visual cortex.
(**B**) Example two-photon image of cholinergic axons in visual cortex.
(**C**) Schematic of the virtual reality system. Mice were head-fixed on a spherical treadmill and surrounded by a toroidal screen on which we presented visual stimuli in different visuomotor conditions.
(**D**) Example trace of the calcium activity of one cholinergic axon in visual cortex (red) and the corresponding locomotion velocity of the mouse (blue).
(**E**) Average locomotion onset activity of all cholinergic axons (5048 axons in 14 mice), sorted by their average response during locomotion onset.
(**F**) Average response of cholinergic axons to locomotion onset over all the cholinergic axons, of the data shown in **E**. Shading indicates SEM over axons. Due to SEM being very small, the shading is fully obscured by the red line.
(**G**) As in **F**, but for grating onsets. Green shading marks the duration of grating presentation.
(**H**) As in **F**, but for visual flow onset during the open loop condition.
(**I**) As in **F**, but for visuomotor mismatch onset. Orange shading marks the duration of visuomotor mismatch. As mismatch events occur only during times of locomotion, and locomotion itself is a strong driver of cholinergic activity, we would expect to find an increase in cholinergic activity by chance at mismatch. To correct for this, we quantified the distribution of cholinergic activity on random triggers during locomotion (95% confidence interval (CI), gray shading).
(**J**) Locomotion onset activity in different visuomotor conditions.
(**K**) The fraction of cholinergic axons responsive to locomotion, grating, and visuomotor mismatch onset, quantified for each imaging site. Each datapoint is one imaging site. Boxes show 25th and 75th percentile, central mark is the median, and the whiskers extend to the most extreme datapoints not considered outliers. Dashed line marks chance level. n.s.: not significant; *: $p < 0.05$; **: $p < 0.01$; ***: $p < 0.001$; see **Table S1** for all statistical information.

acetylcholine levels in visual cortex increased on locomotion onsets (**Figure S2A**), while grating onsets (**Figure S2B**) and visuomotor mismatches (**Figure S2C**) resulted in no measurable increase when corrected for hemodynamic artifacts (**Figures S2A-S2F**). Thus, consistent with previous reports (Larsen et al., 2018), we find that locomotion is associated with a basal forebrain driven increase in acetylcholine levels in visual cortex.

Further characterizing the relationship between locomotion velocity and cholinergic activity, we found that cholinergic axon activity was not linearly related to locomotion velocity, but instead exhibited a locomotion state dependence. Over the course of a locomotion bout, we found that velocity decreased systematically, such that towards the end of a locomotion bout, velocity was lower than at the beginning (**Figure 2A**). For cholinergic activity, this decrease was absent. We found no evidence of a difference in the average calcium activity of cholinergic axons after locomotion onset to that before locomotion offset (**Figure 2B**). Indeed, the average cholinergic activity after locomotion onset and before locomotion offset was highly correlated across locomotion bouts, while a similar analysis on locomotion velocity revealed that the time-course of velocity is more variable and less correlated bout-by-bout (**Figure 2C**). The similarity of locomotion onset and offset responses was not only true for the population average activity, but the activity after locomotion onset, before locomotion offset, and the average activity during the locomotion bout were all well correlated on an axon-by-axon level (**Figures 2D and S2G**). To quantify the relationship between locomotion velocity and calcium activity in cholinergic axons more generally, we computed the average calcium activity as a function of locomotion velocity (see Methods). This relationship was more step-like than linear, and we found no evidence of an increase in calcium activity between low and high locomotion velocities (**Figure 2E**). The same held true for extracellular acetylcholine levels as measured by GRAB-ACh3.0 (**Figure S2H**). If calcium activity in cholinergic axons reflected a step-like change during locomotion, we should find that calcium activity correlates better with a binarized version of locomotion velocity than with locomotion velocity itself. This is indeed what we found (**Figure 2F**), independent of the value of the threshold used for binarization (**Figure S3**). Thus, calcium activity in cholinergic axons in visual cortex is better described as a binary locomotion state signal, than a linear locomotion velocity signal.

A number of behavioral variables, like pupil dilation, facial movements, as well as the overall level of arousal are all correlated with locomotion (Lohani et al., 2022; Reimer et al., 2014; Vinck et al., 2015). It has been shown that cholinergic activity in visual cortex is also well correlated with pupil dilation and facial movements (Larsen et al., 2018; Lohani et al., 2022; Reimer et al., 2014). Disambiguating the effects of locomotion, pupil dilation, and intensity of facial movements on cholinergic activity is complicated by the fact that these three variables are strongly correlated during behavior. It has been shown that under certain conditions, facial movements are a better predictor of cholinergic activity than locomotion across large parts of dorsal cortex (Lohani et al., 2022). To quantify this relationship in visual cortex, we compared the correlation between cholinergic activity, locomotion velocity, pupil diameter, and intensity of facial movements in different visuomotor conditions. This analysis was motivated by our observation that average light levels have a stronger influence on pupil size than locomotion state. We found that the correlation of locomotion velocity and cholinergic activity was independent of visuomotor condition (**Figure 3A**). This was not the case for the correlation between pupil diameter and cholinergic activity, which was systematically lower in darkness than in conditions with visual stimuli, and lower during closed loop visuomotor coupling than during open loop or grating conditions (**Figure 3B**). This pattern was also reflected in the correlation between locomotion and pupil diameter (**Figure 3C**). The reduced correlation between locomotion velocity and pupil diameter in darkness was not a consequence of a decrease in variability due to ceiling-effects in pupil diameter in darkness (**Figure S4A**). Finally, we also computed the correlation between cholinergic activity and facial movements. The correlation of cholinergic activity with locomotion was higher than that with facial movements under all conditions that we

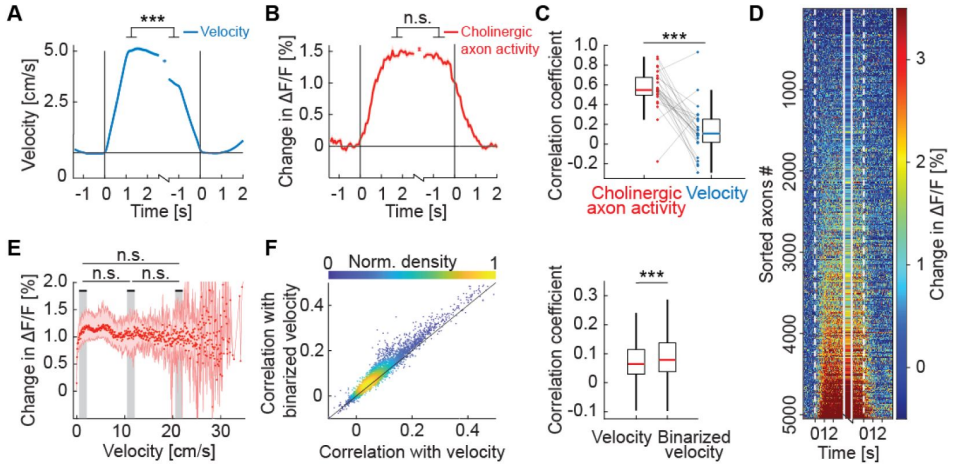

Figure 2.

Activity in cholinergic axons was better explained by a binary locomotion state signal than by locomotion velocity.

(**A**) Average locomotion velocity profiles aligned to locomotion onset and offset. The isolated datapoint between the two traces is the average locomotion velocity over the locomotion bout. Shading marks SEM. Here and elsewhere, n.s.: not significant; *: p<0.05; **: p<0.01; ***: p<0.001; see **Table S1** for all statistical information.
(**B**) As in **A**, but for activity of all cholinergic axons in visual cortex, for the data shown in **D**. Shading marks SEM over axons.
(**C**) Bout-by-bout correlation coefficient between the locomotion onset and offset changes for average cholinergic activity and locomotion velocity. Each datapoint is one imaging site. Boxes show 25th and 75th percentile, central mark is the median, and the whiskers extend to the most extreme datapoints not considered outliers.
(**D**) Average onset and offset responses for all cholinergic axons sorted by strength of locomotion onset response.
(**E**) Activity of cholinergic axons as a function of locomotion velocity. Shown are the hierarchical bootstrap estimates of the median (red dots) and 95% confidence intervals (red shading) for each velocity bin. We found no evidence of a difference in activation between low, intermediate, and high locomotion velocities (indicated by gray shading).
(**F**) Left: For all axons, the correlation coefficient of their calcium activity with locomotion velocity plotted against the correlation coefficient with a binarized version of the locomotion velocity. Right: Distributions of correlation coefficients between calcium activity and locomotion velocity and binarized velocity. Same data as shown on the left. Boxes show 25th and 75th percentile, central mark is the median, and the whiskers extend to the most extreme datapoints not considered outliers.

tested (**Figure S4B**). Thus, of these three behavioral variables, locomotion, pupil diameter, and facial movements, locomotion exhibited the most robust correlation with cholinergic activity in visual cortex (**Figure S4C**).

Next, we turned to the question of what the influence of increased cholinergic activity in visual cortex is on the activity of neurons in layer 2/3 and layer 5. We know that locomotion influences neuronal activity in visual cortex in a variety of ways. One of these effects is that during locomotion, visual responses in visual cortex are increased (Niell and Stryker, 2010) through a combination of both additive and multiplicative effects (Dadarlat and Stryker, 2017). Consistent with this we found locomotion driven increases in visual responses were apparent in both layer 2/3 (**Figure 4A**) and in layer 5 neurons (**Figure 4B**). To test whether this increase in visual responsiveness during locomotion was driven by acetylcholine, we expressed the excitatory opsin ChrimsonR (Klapoetke et al., 2014) in basal forebrain cholinergic neurons using an AAV2/1-hSyn-DIO-ChrimsonR-tdTomato vector in ChAT-IRES-Cre mice. We injected an AAV2/1-Ef1α-GCaMP6f in visual cortex to express GCaMP6f. In cortex, the Ef1α promoter drives highly specific expression in neurons (99.7% of labeled cells in layer 2/3 and 100% of labeled cells in layer 5 are NeuN-positive (Yaguchi et al., 2013)), and biases expression to excitatory neurons, such that approximately 95% of labeled neurons are excitatory in both layer 2/3 (Attinger et al., 2017; Yaguchi et al., 2013) and in layer 5 (Yaguchi et al., 2013). We then performed two-photon calcium imaging in visual cortex to measure the responses of layer 2/3 or layer 5 neurons to the optogenetic activation of local cholinergic axons paired to the presentation of full field drifting grating stimuli while the mouse was stationary (see Methods). We found that in layer 2/3, optogenetic activation of cholinergic axons did not result in a detectable increase in grating onset responses (**Figure 4C**), while the responses of layer 5 neurons to the same stimulus increased with concurrent optogenetic activation of cholinergic axons (**Figure 4D**). The effects of optogenetic activation of cholinergic axons on layer 5 neurons could not be explained by a stimulation triggered change in locomotion velocity (**Figure S5**) or stimulation artifacts (**Figures S6A-S6C**). In mice that did not express ChrimsonR in cholinergic axons (no ChrimsonR controls), we found no evidence of an optogenetic light stimulation effect. Interestingly, this increase in grating onset responses in layer 5 neurons driven by direct cholinergic activation was smaller than that observed during locomotion (**Figures 4B and 4D**). This could be either because the acetylcholine release triggered by the optogenetic stimulation of cholinergic axons was weaker than that occurring during locomotion, or because the increase in responses during locomotion is only partially explained by the co-release of acetylcholine. If the former were the case, we would expect that responses occurring during locomotion are less influenced by optogenetic activation of cholinergic axons. This was indeed the case for grating onset responses during locomotion which were not modulated by optogenetic activation of cholinergic axons (**Figures S6D and S6E**). Interestingly, visuomotor mismatch responses, which also occur only during locomotion, were significantly increased in layer 5 neurons (**Figure 4F**), but not in layer 2/3 (**Figure 4E**). Similarly, we found that optogenetic activation of cholinergic axons increased locomotion onset responses in layer 5 neurons (**Figure 4H**), while layer 2/3 neurons exhibited no significant difference (**Figure 4G**). Thus, while in layer 5 neurons the effect of optogenetic activation appears to saturate for bottom-up grating responses during locomotion, this was not the case for responses that rely on top-down input. However, it is also likely that the increase in response during locomotion is only partially explained by acetylcholine. Locomotion has been shown to result in both a multiplicative and an additive change in grating responses (Dadarlat and Stryker, 2017). This was also the case in our data for locomotion related increase in grating responses (**Figure S7**). However, we found that the optogenetic stimulation of cholinergic axons resulted primarily in a multiplicative gain of visual responses (**Figure S7**). Overall, consistent with previous findings (Goard and Dan, 2009), we find that acetylcholine primarily increases both bottom-up and top-down driven responses in layer 5 but not layer 2/3 neurons, but only partially explains the locomotion driven increases in visual responses.

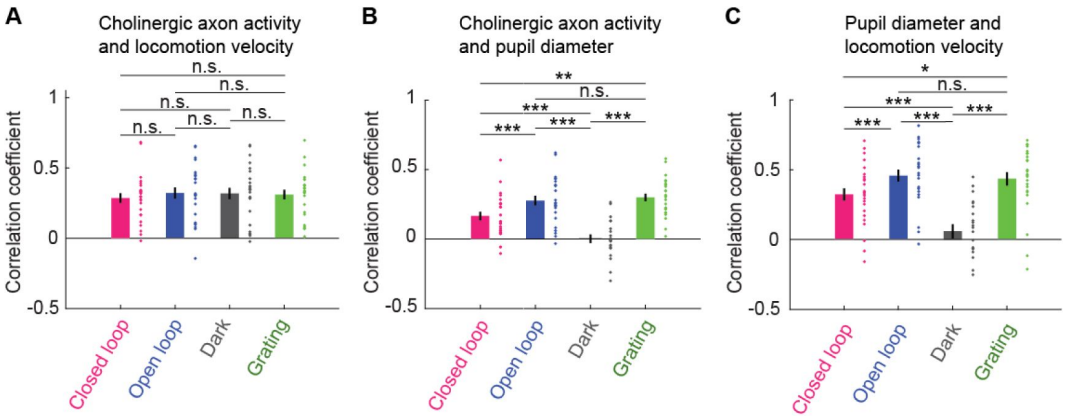

Figure 3.

Average activity of cholinergic axons was more strongly correlated with locomotion velocity than with pupil diameter.

(**A**) Correlation of average activity of cholinergic axons activity with locomotion velocity in closed loop, open loop, dark, and grating conditions. Each point represents data from one imaging site, error bars indicate SEM. Here and elsewhere, n.s.: not significant; *: $p < 0.05$; **: $p < 0.01$; ***: $p < 0.001$; see **Table S1** for all statistical information.
(**B**) As in **A**, but for correlation between average activity of cholinergic axons and pupil diameter.
(**C**) As in **A**, but for correlation between locomotion velocity and pupil diameter.

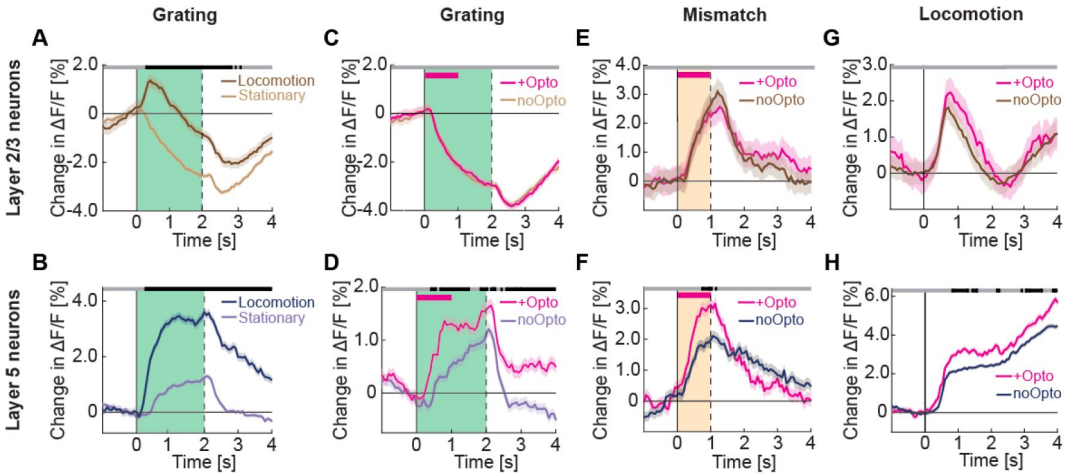

Figure 4.

Optogenetic activation of cholinergic axons in visual cortex primarily enhances responses of layer 5, but not layer 2/3 neurons.

(**A**) Average calcium response of layer 2/3 neurons in visual cortex to full field drifting gratings in the absence (light brown) or presence of locomotion (brown). Green shading indicates duration of grating stimulus. The responses are compared bin-by-bin using a nested hierarchical bootstrap test. Here and in subsequent panels, bins with a significant difference ($p < 0.05$) are indicated by a black line above the plot; those with $p > 0.05$ are marked gray. Shading marks SEM.
(**B**) As in **A**, but for layer 5 neurons in visual cortex in the absence (light blue) or presence (dark blue) of locomotion.
(**C**) Average calcium response of layer 2/3 neurons in visual cortex to full field drifting gratings while the mice were stationary, without (light brown) or with (pink) optogenetic activation of cholinergic axons in visual cortex. Duration of optogenetic stimulation is marked by a pink bar. Green shading indicates duration of the grating stimulus.
(**D**) As in **C**, but for layer 5 neurons in visual cortex.
(**E**) Average calcium response to visuomotor mismatch in layer 2/3 neurons in visual cortex, without (brown) and with (pink) optogenetic stimulation of cholinergic axons in visual cortex. Orange shading indicates mismatch duration, and pink bar indicates optogenetic stimulation.
(**F**) As in **E**, but for layer 5 neurons in visual cortex.
(**G**) Average calcium response of layer 2/3 neurons in visual cortex to locomotion onset in closed loop, without (brown) or with (pink) optogenetic stimulation of cholinergic axons in visual cortex.
(**H**) As in **G**, but for layer 5 neurons in visual cortex.

A second effect of locomotion on neuronal activity in visual cortex is that locomotion itself drives neuronal responses (Keller et al., 2012; Saleem et al., 2013). This effect is apparent in both layer 2/3 (**Figure 5A**) and layer 5 (**Figure 5B**) neurons. In layer 2/3, locomotion related activity is suppressed by closed loop visual feedback (Widmer et al., 2022), as a function of the strength of visuomotor mismatch responses (**Figure S8A and S8B**). In layer 5, closed loop visual feedback did not suppress running related activity on average in either visuomotor mismatch or grating responsive neurons (**Figure S8C and S8D**). Thus, locomotion related activity likely has functionally distinct roles in layer 2/3 and layer 5. To test whether artificial activation of cholinergic axons would result in increased neuronal activity, we again performed two-photon calcium imaging in visual cortex neurons to measure responses of layer 2/3 or layer 5 neurons upon optogenetic activation of local cholinergic axons. We found no evidence of any increase in calcium activity in either layer 2/3 (**Figure 5C**) or layer 5 neurons (**Figure 5D**). This absence of a stimulation response is consistent with previous reports that found that cholinergic axon stimulation in visual cortex does not result in a response of layer 2/3 neurons (Chen et al., 2015) and that electrical stimulation of basal forebrain primarily activates inhibitory neurons in superficial layers of visual cortex (Alitto and Dan, 2012). This, combined with our finding that on average the layer 2/3 locomotion onset related activity preceded the activity increase in cholinergic axons (**Figure S1**), would indicate that the locomotion related increase in layer 2/3 and layer 5 activity observed in visual cortex is not driven by acetylcholine.

A third effect locomotion has on neuronal activity in visual cortex is to decorrelate the activity of nearby neurons (Dadarlat and Stryker, 2017; Erisken et al., 2014). Consistent with these studies, we found that locomotion results in a reduction of pairwise correlations between activity of layer 2/3 neurons (**Figures 6A and 6E**) as well as between layer 5 neurons (**Figures 6B and 6F**). We could induce this decorrelation by optogenetically activating the cholinergic axons while mice were stationary. This optogenetically induced decorrelation in layer 2/3 (**Figures 6C and 6E**) was stronger than that driven by locomotion, while the two were similar in layer 5 (**Figures 6D and 6F**). Note, we used calcium activity of apical dendrites of L5 neurons in L2/3 as a proxy for somatic L5 activity in these experiments (see Methods). This decorrelation was not due to a visual response to the stimulation laser (**Figure S6F**). Interestingly, we found that in both layer 2/3 and layer 5, the locomotion induced decorrelation was observed primarily for neurons with low pairwise correlations. Pairs of neurons with high correlation of activity tended to further increase their correlation during locomotion (**Figure S9**). Finally, we tested whether the correlation in visual cortex was similarly influenced by chemogenetic manipulation of basal forebrain cholinergic neurons. We expressed either a DREADD activator or a DREADD inhibitor in ChAT-Cre mice to systemically increase or decrease cholinergic activity. Interestingly, we noticed that the systemic increase or decrease of cholinergic release resulted in behavioral changes in the mice. Upon chemogenetic activation mice increased their locomotion velocity, and upon chemogenetic inhibition, mice decreased their time spent locomoting, resulting in a bidirectional modulation of the total distance traveled by the two manipulations (**Figure S10**). Importantly, chemogenetic manipulations bidirectionally modulated the decorrelation effect on locomotion in layer 5 neurons in visual cortex. DREADD activation resulted in an increased strength of the locomotion driven decorrelation, while DREADD inhibition resulted in a reduced strength of locomotion driven decorrelation in layer 5 (**Figures 6H and S11B**). This effect was absent in layer 2/3 where neither manipulation influenced the locomotion driven decorrelation (**Figures 6G and S11A**). Thus, cholinergic activation is likely sufficient to explain the locomotion induced decorrelation of activity in visual cortex.

Finally, an effect of locomotion on the responses of layer 5 neurons, which to the best of our knowledge is unreported, is a decrease in latency to response. In layer 5 neurons, responses to grating stimuli appeared earlier during locomotion than they did while the mouse was stationary (**Figures 4B and 7B**). This decrease in response latency during locomotion was absent in layer 2/3 neurons (**Figures 4A and 7A**). Optogenetic activation of cholinergic axons was able

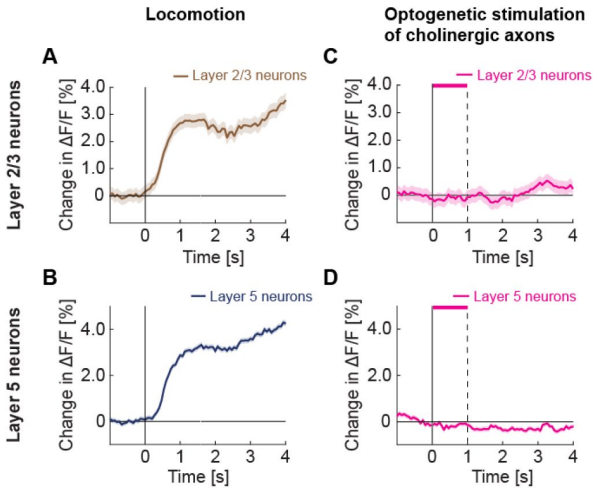

Figure 5.

Optogenetic activation of cholinergic axons in visual cortex did not drive responses in either layer 2/3 or layer 5 neurons.

(**A**) Average calcium response of layer 2/3 neurons in visual cortex to locomotion onset in open loop. Shading indicates SEM.
(**B**) As in **A**, but for layer 5 neurons in visual cortex.
(**C**) Average calcium response of layer 2/3 neurons in visual cortex during local optogenetic stimulation of cholinergic axons while the mice were stationary. Pink bar marks duration of the optogenetic stimulus.
(**D**) As in **C**, but for layer 5 neurons in visual cortex.

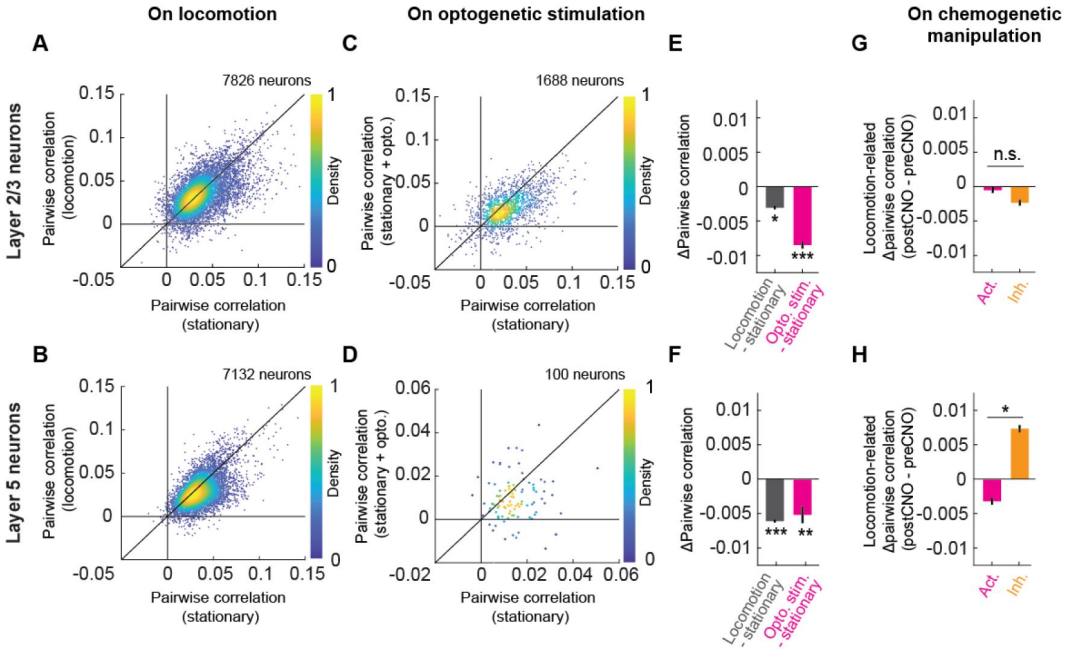

Figure 6.

Cholinergic axon activation reduced pairwise correlations between neurons in visual cortex.

(**A**) Average pairwise correlation in calcium activity of layer 2/3 neurons while the mouse was stationary and while the mouse was locomoting. Each dot is the mean of the pairwise correlations for one neuron to all others in the same field of view.
(**B**) As in **A**, but for layer 5 neurons.
(**C**) As in **A**, but comparing the correlation while the mice were stationary, to that while cholinergic axons were stimulated optogenetically.
(**D**) As in **C**, but for layer 5 neurons. Note, for this experiment the imaging plane was in L2/3 to simultaneously image layer 2/3 neurons and apical dendrites of layer 5. The latter were traced to their soma in layer 5 offline and were used to compute layer 5 activity correlations.
(**E**) Average change in pairwise correlations of layer 2/3 neurons on locomotion (gray) or on optogenetic stimulation of cholinergic axons during stationary periods (pink), compared to the correlations during stationary (stat.) periods at baseline. Here and elsewhere, n.s.: not significant; *: $p < 0.05$; **: $p < 0.01$; ***: $p < 0.001$; see **Table S1** for all statistical information.
(**F**) As in **E**, but for layer 5 neurons of visual cortex.
(**G**) Change in the average pairwise correlations of layer 2/3 neurons during locomotion, upon DREADD activation (pink) or inhibition (orange) of basal forebrain cholinergic neurons.
(**H**) As in **G**, but for layer 5 neurons.

to recapitulate the decrease in response latency in layer 5 neurons (**Figures 4D**, **7B** and **S12B**), while leaving layer 2/3 neuron response latency unaffected (**Figures 4C**, **7A** and **S12A**). Thus, cholinergic input decreases the response latency of layer 5 neurons.

Discussion

We set out to address the question of why acetylcholine is released in visual cortex by answering two simpler, intermediate questions: what drives acetylcholine release, and what immediate effects does the released acetylcholine have on the cortical circuits. We found that locomotion was the main driver of ChAT axons activity (**Figure 1**) and acetylcholine release (**Figure S2**) in visual cortex, and cholinergic activity depended on locomotion velocity in a non-linear, step-like manner (**Figure 2**). The acute effects of this increase in acetylcholine on cortical responses were layer-specific: acetylcholine release enhanced responses specifically in layer 5 neurons, but not in layer 2/3 (**Figure 4**). Using chemogenetic manipulations of basal forebrain cholinergic neurons, we found that we could bidirectionally influence the activity correlations of layer 5 neurons. Cholinergic activation resulted in a decrease of pairwise correlations while inhibition resulted in an increase (**Figure 6H**). We observed a similar decrease in pairwise correlations during optogenetic stimulation of cholinergic axons in visual cortex, arguing that this effect is, at least in part, mediated locally (**Figure 6F**). Similarly, optogenetic stimulation of cholinergic axons in visual cortex drove a decrease in pairwise correlation of layer 2/3 (**Figure 6E**), while global manipulation of the basal forebrain cholinergic system using chemogenetic tools did not significantly change correlations on activation or inhibition (**Figure 6G**). Our results would be consistent with the interpretation that the acute effects of acetylcholine are stronger in layer 5 where they act to increase responsiveness to inputs from outside of the local layer 5 network.

While the optogenetic activation of cholinergic axons in visual cortex likely recapitulates the local effects of acetylcholine more directly than those observed with basal forebrain stimulation, the method comes with the following caveats. First, we don't know how the pattern of acetylcholine release induced by optogenetic activation of cholinergic axons compares to that observed endogenously during locomotion. The pattern of cholinergic axon activation was not uniform across axons (**Figures 1E and 2D**), consistent with different modes of activity in cholinergic subpopulations observed in basal forebrain (Laszlovszky et al., 2020). It is unclear whether the exact pattern of cholinergic axon activation substantially influences the observed effects in cortex. However, given that the effects on changes in the correlation of activity induced by optogenetic activation of cholinergic axons was at least as strong as that observed during locomotion, we estimate that optogenetic activation of cholinergic axons can induce levels and patterns of acetylcholine release similar to those observed endogenously. Second, the activation of cholinergic axons likely antidromically activates cholinergic neuron soma in basal forebrain. Thus, we cannot exclude the possibility of a systemic contribution to the effects we observe through shared projections between different cortical and subcortical targets. However, the projection specificity of basal forebrain cholinergic neurons (Kim et al., 2016; Pinto et al., 2013) would argue against this. Finally, it is important to note that here we labeled basal forebrain cholinergic neurons with targeted viral injection. Thus, we cannot exclude the possibility that our labelling of cholinergic axons was incomplete. The alternative approach to label these neurons by crossing ChAT-Cre mice to a reporter line expressing a calcium indicator comes with the caveat of the presence of a substantial fraction of VIP interneurons in visual cortex that also are ChAT positive (Granger et al., 2020). Being unable to separate basal forebrain axons from those of local VIP interneurons complicates the interpretation of results.

Another caveat of our conclusions is the fact that our neuronal populations in both layer 2/3 and layer 5 are not random subsets. While the Ef1α promoter is specific to neurons (Tsuchiya et al., 2002; Yaguchi et al., 2013) and predominantly labels excitatory neurons (Attinger et al., 2017; Yaguchi et al., 2013), the expression levels are likely not equal across the different

excitatory neuron types. In layer 5, for example, we are likely undersampling Tlx3-positive layer 5 neurons. Tlx3-positive layer 5 neurons exhibit a visually driven reduction in activity and consequently have a systematic difference between open and closed loop locomotion onsets (Heindorf and Keller, 2022). We do not see either a visually driven inhibition on average (**Figure 4D**), nor a difference between closed and open loop locomotion onsets (**Figure S8**). Thus, it should be kept in mind that with any virus based protein expression, the population of labeled cells is likely not random genetically, and that descriptor of 'layer 2/3 (or 5) neuron' should be understood to mean, a 'layer 2/3 (or 5) neuron that exhibits high expression levels under the artificial Ef1α promoter when used in an AAV delivery vector'.

Given our results, what are the implications for the computational role of acetylcholine in visual cortex? There are likely two aspects to this, the acute effect on cortical activity and the effect on plasticity. We find that acetylcholine was released in visual cortex as a locomotion state signal. This state signal could be used to gate visuomotor plasticity. In systems engaged in sensorimotor learning, plasticity related to feedback prediction errors should occur primarily during self-motion and not when passively experiencing sensory input. Visuomotor development is critically dependent on coupling of locomotion and sensory feedback (Attinger et al., 2017; Held and Hein, 1963; Kaneko and Stryker, 2014), and depends on local plasticity mechanisms in visual cortex (Widmer et al., 2022). Acetylcholine is known to gate plasticity in visual cortex (Bear and Singer, 1986; Greuel et al., 1988; Gu and Singer, 1993; Kirkwood et al., 1999) and could function to gate visuomotor plasticity to phases of self-motion. Given that acetylcholine release is associated with other types of movement as well (Eggermann et al., 2014; Harrison et al., 2016; Lohani et al., 2022; Nelson and Mooney, 2016; Zhu et al., 2023), this is consistent with acetylcholine functioning more generally as a movement state signal. We would predict that in visual cortex, this would primarily relate to movements that result in changes to visual input.

The absence of an acute effect of optogenetically stimulating cholinergic axons locally on activity of visual cortex neurons is consistent with the idea that locomotion driven neuronal activity in visual cortex (Keller et al., 2012; Saleem et al., 2013) is likely not driven by acetylcholine, but is the consequence of a combination of motor-related top-down input (Leinweber et al., 2017) and noradrenaline (Polack et al., 2013), another neuromodulator that is known to accompany locomotion onset (Jordan and Keller, 2023; Reimer et al., 2016). Consistent with previous reports (Goard and Dan, 2009), we find that acetylcholine acutely increases visuomotor responses more strongly in layer 5 neurons than in layer 2/3 neurons and that it decorrelates neuronal activity. One of the key questions here is why these effects are induced during locomotion. There are a number of explanations that have been proposed previously that often focus on increasing sensory gain to counteract the noisier visual input during locomotion (Minces et al., 2017; Pinto et al., 2013). We propose a slightly more specific explanation. This is based on the idea that the observed effects of acetylcholine on layer 5 can be explained by assuming the layer 5 network exhibits attractor dynamics and that acetylcholine modifies these attractor dynamics (Kanamaru and Aihara, 2019). The observed differences in the effect of acetylcholine on layer 5, where response strength increased, and layer 2/3, where they did not, are consistent with the interpretation that attractor dynamics are stronger in layer 5 than in layer 2/3. This would, also agree with a proposed microcircuit for predictive processing (Keller and Mrsic-Flogel, 2018), where layer 5 is postulated to maintain an internal representation (Heindorf and Keller, 2022). Thus, acetylcholine could act to increase the sensitivity and speed of response of the internal representation neurons to inputs arriving from outside the local network at the expense of reducing the influence among neurons in the local network. Such an acetylcholine driven increase in the speed of transition between different internal representations would also be consistent with the finding that layer 5 neurons exhibit faster responses to the transitions between different stimuli (**Figure 7**). Assuming the internal representation in cortex is a substrate of conscious perception, as proposed by predictive processing, this would be consistent with the finding that anesthesia decouples layer 5 neurons from their inputs onto apical dendrites by cholinergic mechanisms (Suzuki and Larkum, 2020).

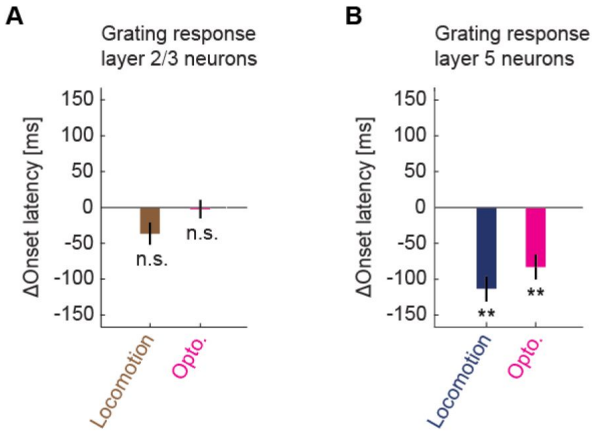

Figure 7.

Cholinergic input reduced response latency of layer 5 neurons in visual cortex to grating stimuli.

(**A**) Locomotion (brown) or optogenetic stimulation of cholinergic axons (pink) induced change in the response latency of layer 2/3 neurons in visual cortex to full field drifting grating onset. Here and elsewhere, n.s.: not significant; *: p<0.05; **: p<0.01; ***: p<0.001; see **Table S1** for all statistical information.
(**B**) As in **A**, but for layer 5 neurons.

What makes this hypothesis all the more tantalizing is the observation that a decrease in cortical cholinergic activation is correlated with the severity of dementia in Alzheimer's disease (Perry et al., 1978). All three drugs currently approved for the management of dementia in Alzheimer's disease are cholinesterase inhibitors, drugs that increase acetylcholine levels. If cholinergic activation alters network dynamics to make the putative layer 5 attractor network more sensitive to external inputs – and hence more easily influenced by long-range cortical inputs – this could explain why cholinergic activation enhances memory retrieval. A decrease in cholinergic tone in Alzheimer's disease is also consistent with the increases of correlation of neuronal activity in cortex observed in mouse models of the disease (Korzhova et al., 2021). Thus the cholinergic gating of the sensitivity of layer 5 to external inputs could constitute a possible mechanism for the cholinergic hypothesis for Alzheimer's disease (Davies and Maloney, 1976; Francis et al., 1999; Hampel et al., 2019; Terry and Buccafusco, 2003).

In summary, we show that cholinergic activity in visual cortex conveys a locomotion state signal, that preferentially augments the response of layer 5 neurons to external inputs and decorrelates activity across neurons, possibly to both sculpt the receptive field tuning of neurons to sensory stimuli as well as to regulate the influence of external input on internal representation to affect our conscious percept.

Methods

Key Resources Table

REAGENT or RESOURCE	Source	Identifier
Bacteria and Virus Strains		
AAV2/5-hSyn1-FLEx-axon-GCaMP6s (10^{13}-10^{15} GC/ml)	FMI vector core	vector.fmi.ch
AAV PHP.eB-Ef1α-DIO-GCaMP6s (10^{11} GC/ml)	FMI vector core	vector.fmi.ch
AAV2/1-hSyn-DIO-ChrimsonR-tdTomato (10^{11}-10^{13} GC/ml)	FMI vector core	vector.fmi.ch
AAV2/1-Ef1α-GCaMP6f-WPRE (10^{11}-10^{14} GC/ml)	FMI vector core	vector.fmi.ch
AAV2/1-Ef1α-DIO-hM3D(Gq)-mCherry (10^{11} GC/ml)	FMI vector core	vector.fmi.ch
AAV2/1-Ef1α-DIO-hM4D(Gi)-mCherry (10^{11} GC/ml)	FMI vector core	vector.fmi.ch
AAV2/9-hSyn-GRAB-ACh3.0 (10^{13} GC/ml)	FMI vector core	vector.fmi.ch
AAV2/1-Ef1α-DIO-tdTomato-WPRE (10^{14} GC/ml)	FMI vector core	vector.fmi.ch
AAV2/1-Ef1α-GFP-WPRE (10^{12} GC/ml)	FMI vector core	vector.fmi.ch
Chemicals, Peptides, and Recombinant Proteins		
CNO	Tocris	Cat# 4936-10mg
Fentanyl citrate	Actavis	CAS 990-73-8
Midazolam (Dormicum)	Roche	CAS 59467-96-8
Medetomidine (Domitor)	Orion Pharma	CAS 86347-14-0
Ropivacaine	Presenius Kabi	CAS 132112-35-7
Lidocaine	Bichsel	CAS 137-58-6
Buprenorphine	Reckitt Benckiser Healthcare	CAS 52485-79-7
Ophthalmic gel (Humigel)	Virbac	-
Flumazenil (Anexate)	Roche	CAS 78755-81-4
Atipamezole (Antisedan)	Orion Pharma	CAS 104054-27-5
N-Butyl-2-cyanoacrylate (Histoacryl)	Braun	CAS 6606-65-1
Dental cement (Paladur)	Heraeus Kulzer	CAS 9066-86-8
Deposited data		
All data and code used to generate manuscript figures	This paper	data.fmi.ch
Experimental Models: Organisms/Strains		
Mus musculus: C57BL/6	Charles River	-
Mus musculus: B6J.129S6-Chat$^{tm2(Cre)Lowl}$/MwarJ	Jackson Laboratories	RRID:IMSR_JAX:028861
Software and algorithms		
MATLAB (2020b)	The MathWorks	RRID:SCR_001622
LabVIEW	National Instruments	RRID:SCR_014325
Two-photon acquisition software	Keller laboratory	sourceforge.net/p/iris-scanning/
Image data processing software	Keller laboratory	sourceforge.net/p/iris-scanning/calliope
Python	python.org	RRID:SCR_008394
Panda3D	panda3d.org	N/A
Other		

Virtual reality and two-photon setup	(Leinweber et al., 2014, 2017)	DOI: 10.3791/50885, 10.1016/j.neuron.2017.08.036
Optogenetic stimulation laser (OBIS 673 nm LX)	Coherent	Cat#1187194
Sham stimulation LED	Prizmatix	UHP-T-595
Titanium headplate	FMI/ETHZ workshop	N/A
Dental drill	Meisinger	N/A

Mice

All mice used in experiments described in the paper were ChAT-IRES-Cre (Rossi et al., 2011) heterozygotes, kept on a C57BL/6 background. A total of 64 mice, both male and female, 6-16 weeks old at the start of the experiment, were used. See **Table S2** for details of mouse inclusion for the different figures. Between experiments, mice were group-housed in a vivarium (light/dark cycle: 12/12 hours). All animal procedures were approved by and carried out in accordance with the guidelines laid by the Veterinary Department of the Canton of Basel-Stadt, Switzerland.

Surgery

For all surgical procedures, mice were anesthetized with a mixture of fentanyl (0.05 mg/kg; Actavis), midazolam (5.0 mg/kg; Dormicum, Roche), and medetomidine (0.5 mg/kg; Domitor, Orion) injected intraperitoneally. Analgesics were applied perioperatively (2% lidocaine gel, meloxicam 5 mg/kg) and postoperatively (buprenorphine 0.1 mg/kg, meloxicam 5 mg/kg). Eyes were covered with ophthalmic gel (Virbac Schweiz AG). Cranial windows were implanted as previously described (Keller et al., 2012; Leinweber et al., 2014). Briefly, using a dental drill, a 4 mm craniotomy was made over the right visual cortex, centered 2.5 mm lateral and 0.5 mm anterior to lambda. After injection of AAV vectors, the exposed cortex was sealed with a 4 mm circular glass coverslip and glued in place using gel superglue (Ultra Gel, Pattex). The remaining exposed surface of the skull was covered with Histoacryl (B. Braun), and a titanium head bar was fixed to the skull using dental cement (Paladur, Heraeus Kulzer). After surgery, anesthesia was antagonized by a mixture of flumazenil (0.5 mg/kg; Anexate, Roche) and atipamezole (2.5 mg/kg; Antisedan, Orion Pharma) injected intraperitoneally.

Axonal labeling

To image the activity of basal forebrain cholinergic axons in visual cortex, we expressed a calcium indicator in basal forebrain cholinergic neurons. Surgery was performed as described above, and either an AAV2/5-hSyn1-FLEx-axon-GCaMP6s (10^{13} GC/ml) or an AAV-PHP.eB-Ef1α-DIO-GCaMP6s (10^{12} GC/ml) was injected at four locations ipsilateral to the imaging site (AP, ML, DV (in mm): +1.1, +0.1, −3.7 (medial septum); +1.1, +0.1, −4.1 (vertical limb of the diagonal band); +0.8, +0.1, −4.2 (horizontal limb of the diagonal band); +0.6, +0.6, −4.9 (nucleus basalis)) in ChAT-IRES-Cre mice.

GRAB imaging

We injected an AAV vector carrying GRAB-ACh 3.0, AAV2/9-hSyn-GRAB-ACh3.0 (10^{13} GC/ml), in visual cortex. A 4 mm craniotomy was made over right visual cortex and sealed with a glass coverslip as described above.

Chemogenetic experiments

To manipulate the activity of the basal forebrain cholinergic system, we used chemogenetic DREADD inhibitor AAV2/1-EF1α-DIO-hM4D(Gi)-mCherry (10^{11} GC/ml) or DREADD activator AAV2/1-EF1α-DIO-hM3D(Gq)-mCherry (10^{11} GC/ml). AAVs were injected in anterior basal forebrain with coordinates as used for axonal imaging described above. DREADDs were stimulated using Clozapine N-oxide (CNO), which was dissolved in DMSO, diluted with saline, and injected intraperitoneally at a dose of 0.5 mg/kg body weight. Activity from each imaging site in the DREADD series was acquired starting 30 min - 60 min after CNO injection.

Optogenetic experiments

We injected AAV2/1-hSyn-DIO-ChrimsonR-tdTomato (10^{11} GC/ml) into basal forebrain at the same coordinates as for axonal imaging described above, and injected AAV2/1-Ef1α- GCaMP6f-WPRE ($10^{11\text{-}14}$ GC/ml) into visual cortex for imaging neurons in layer 2/3 and layer 5. In no-opsin control mice, instead of ChrimsonR, we injected an AAV2/1-DIO-tdTomato-WPRE (10^{14} GC/ml) virus. ChrimsonR stimulation and functional imaging of GcaMP6f-expressing neurons was done as

previously described (Attinger et al., 2017). For imaging, we used a modified Thorlabs B-Scope with a 12 kHz resonance scanner (Cambridge Technology). The illumination source for the optogenetic stimulation was a 637nm laser (OBIS LX, Coherent). We used a dichroic mirror (ZT775sp-2p, Chroma) to combine the two-photon laser and stimulation laser. A second long-pass dichroic mirror (F38-555SG, Semrock) was used to split the GCaMP emission from both illumination light sources. Light leak from the 637 nm stimulation laser was reduced by synchronizing the stimulation laser to the turnaround times of the resonant scanner (during which imaging data were not acquired). Lastly, amplified PMT signals were digitally bandpass filtered at 80 MHz to reduce the effect of ringing in the amplifier. This allowed for near stimulation-artifact free synchronous imaging and optogenetic stimulation. For all experiments with stimulation of cholinergic axons locally in visual cortex, we used a square-wave pulse of 1s duration and 10 mW/mm^2 power (measured at objective). The median inter-trial interval for different stimulation events was 15 s for optogenetic stimulation only trials, 12 s for optogenetic stimulation with grating onset, 35 s for optogenetic stimulation with visuomotor mismatch, and 45 s for optogenetic stimulation with locomotion onset in closed loop. To measure correlation changes, we employed a longer laser stimulation window of 1 minute, at 40 Hz (50% duty cycle), with an average power output of 20 mW/mm^2 (measured at objective). For sham stimulation, we used an optical guide coupled to a high-power LED (UHP-T-595, Prizmatix) to diffusely illuminate the mouse and surrounding virtual reality setup.

Virtual reality environment

The virtual reality setup is based on the design of Dombeck and colleagues (Dombeck et al., 2007). Briefly, mice were head-fixed and free to run on an air-supported spherical treadmill. The rotation of the ball was restricted around the vertical axis with a pin. The virtual reality environment was projected onto a toroidal screen covering approximately 240 degrees horizontally and 100 degrees vertically of the mouse's visual field, using a projector (Samsung SP-F10M) synchronized to the resonant scanner of the two-photon microscope. The virtual environment consisted of an infinite corridor with walls patterned with vertical sinusoidal gratings with a spatial frequency of approximately 0.04 cycles per degree (Leinweber et al., 2014). In closed loop condition, the locomotion of the mouse was coupled to movement along a virtual tunnel. In open loop condition, we uncoupled the two and replayed the visual flow from a preceding closed loop condition. In grating condition, we presented full field drifting gratings (0°, 45°, 90°, 270°, moving in either direction) in a pseudo-random sequence. Grating stimuli were presented for between 2 s and 3 s. In the inter-stimulus interval (between 2 s and 4 s), mice were shown a gray screen with average luminance matched to that of the grating stimuli.

Eye tracking and facial movement measurement

During all experiments, we recorded the mouse's left eye (contralateral to the imaged hemisphere) with a CMOS infrared camera at 30 Hz frame rate. The pupil was backlit by the 930 nm laser used for two-photon imaging. We calculated pupil diameter offline by fitting a circle to the pupil. Frames with occluded pupil were excluded from analysis. To extract facial movements, we computed the average image displacement in different image patches on the face of the mouse.

Two-photon microscopy

Functional two-photon calcium imaging was performed using custom-built two-photon microscopes (Leinweber et al., 2014). The illumination source was a tunable femtosecond laser (Insight, Spectra Physics or Chameleon, Coherent) tuned to 930 nm. Emission light was band-pass filtered using a 525/50 filter for GCaMP and a 607/70 filter for tdTomato/mCherry (Semrock) and detected using a GaAsP photomultiplier (H7422, Hamamatsu). Photomultiplier signals were amplified (DHPCA-100, Femto), digitized (NI5772, National Instruments) at 800 MHz, and band-pass filtered at 80 MHz using a digital Fourier-transform filter implemented in custom-written software on an FPGA (NI5772, National Instruments). The scanning system of the microscopes was

based either on a 12 kHz or an 8 kHz resonant scanner (Cambridge Technology). Images were acquired at a resolution of 750 x 400 pixels (60 Hz or 40 Hz frame rate, respectively), and a piezo-electric linear actuator (P-726, Physik Instrumente) was used to move the objective (Nikon 16x, 0.8 NA) in steps of 15 µm between frames to acquire images at 4 different depths. This resulted in an effective frame rate of 15 Hz or 10 Hz, respectively. The field of view was 375 µm x 300 µm.

Extraction of neuronal activity

Calcium imaging data were processed as previously described (Keller et al., 2012) and all data analysis was done in MATLAB (MathWorks). Briefly, raw images were full-frame registered to correct for lateral brain motion. Neurons and axons were manually selected based on mean and maximum fluorescence images. For GRAB imaging, neuropil and blood vessels were manually selected. For a subset of mice, the apical dendrites of layer 5 neurons were marked in layer 2/3 by manually tracing them to their soma in layer 5 using a z-stack acquired at the end of an experiment. Raw fluorescence traces were corrected for slow drift in fluorescence using an 8^{th}-percentile filtering with a 66 s (or 1000 frames) window (Dombeck et al., 2007). ΔF/F traces were calculated as mean fluorescence in a selected region of every imaging frame, subtracted and normalized by the overall median fluorescence. All neuronal calcium activity data was acquired at 15 Hz. For axonal imaging, 9 (of 25 sites) were imaged at 10 Hz, and analytically resampled at 15 Hz using a polyphase antialiasing filter to make the time-base compatible with the rest of the axonal imaging data.

Data analysis

All data analysis was done using custom scripts written in MATLAB (MathWorks). To quantify the average population response traces, we first calculated the average event-triggered fluorescence trace for each region of interest (ROI). The responses of all ROIs was then averaged and baseline-subtracted.

Locomotion onset was defined as locomotion velocity crossing a threshold of 0.25 cm/s for at least 1 s, while having been below the threshold for 1 s before. The same criteria were used to define visual flow onsets in the open loop condition using visual flow speed. Visuomotor mismatch responses were probed by presenting brief 1 s full field visual flow halts in the closed loop condition. For a mismatch event to be included in analysis, mice had to be locomoting uninterrupted above threshold (0.25 cm/s) from −0.5 s to +1 s after the event onset. Additionally, for a ROI to be included for analysis of the response to a particular event, it had to have at least 5 onsets to the event.

In **Figure 1E**, the calcium responses were baseline subtracted using a −1 s to −0.5 s window relative to locomotion onset and sorted based on the average response in the +0.5 s to +1.5 s activity window. In **Figures 1F-1H**, the activity was averaged over all axons, with a baseline subtraction window of −1 s to −0.5 s relative to onset. In **Figure 1I**, the baseline window was −0.5 s to 0 s relative to mismatch onset (to include the locomotion related response in the baseline), and a 95% confidence interval was calculated from randomly drawn timepoints during locomotion. In **Figure 1J**, the locomotion onset response is plotted across different visuomotor conditions, and the baseline window was −1 s to −0.5 s. In **Figure 1K**, cholinergic axons ware classified as responsive to a particular stimulus if the mean activity in a window +0.5 s to +1.5 s after stimulus onset was significantly different (paired two-sample t-test over onsets, $p < 0.05$) from the mean of the baseline window (−1 s to −0.5 s).

Locomotion offset was defined as the threshold crossing at which locomotion velocity decreased below 0.25 cm/s for at least 1 s after mice ran above the threshold for at least 1 s. To isolate locomotion bouts, we identified consecutive locomotion onset and offset events that were separated by at least 4 s. In **Figure 2C**, we computed correlations in average calcium activity (or locomotion velocity) between locomotion onset and offset across locomotion bouts. Onset

responses were defined as the average population activity (or locomotion velocity) +0.5 s to +1.5 s after locomotion onset with a baseline of −1 s to −0.5 s. Offset responses were similarly defined as the average population activity (or locomotion velocity) over - 1.5 s to −0.5 s before locomotion offset with the same baseline as for bout onset. In **Figure 2D**, axons were sorted based on their average activity at locomotion onset (defined as above), and the same sort order was preserved for plotting the average activity during the bout and at bout offset. In **Figure 2E**, locomotion velocity was binned into 100 evenly spaced bins in the range of 0 cm/s to 6.25 cm/s, and the activity of cholinergic axons in each bin was averaged. In **Figure 2F**, the correlation of the activity of each cholinergic axon was computed against the mouse locomotion velocity, and this was compared against the correlation computed with a binarized version of locomotion velocity, binarized using a threshold of 0.25 cm/s.

In **Figures 3B**, **3C** **and S4B** with pupil data, we excluded frames with blinks. For variability and correlation analysis involving pupil diameter, sites with less than 30 s of pupil data in a visuomotor condition were excluded.

In **Figures 4A-4H**, to probe for the influence of cholinergic stimulation on responses in visual cortex, the optogenetic stimulation laser was turned on for 1 s coincident with the onset of mismatch or grating stimuli. Further, to isolate the influence of cholinergic stimulation based on the locomotion state, an instance of grating stimulus presentation was defined as occurring during 'locomotion' if mice had a locomotion velocity that was above a threshold (0.25 cm/s) in the time-window of −0.5 s to +1 s from the stimulus onset, otherwise it was defined as occurring while the mouse was 'stationary'. Note, the same criteria to define locomotion state was used to isolate visuomotor mismatches, and also during control optogenetic stimulation experiments (**Figures S6A-S6E**). For stimulation on locomotion onset, we detected locomotion onsets based on locomotion velocity in real-time. The average delay between locomotion onsets and laser stimulation onsets was 406 ms ± 41 ms (mean ± SEM).

In **Figure S7**, for each neuron, we determined the preferred orientation using half the trials while the mice were stationary, and plotted responses relative to this preferred orientation in the other half of the stationary trials, or while the mice were locomoting, or during optogenetic stimulation of cholinergic axons while stationary. As before, a velocity threshold of 0.25 cm/s was used to separate stationary trials from locomoting.

In **Figures 6A-6F**, to compute the average pairwise correlation in activity of neurons, we first split the activity trace based on the locomotion state of the mouse and the presence of optogenetic stimulation. Then, for each condition, we computed the average over all pairwise correlations of a given neuron with every other neuron from the same imaging site. For the chemogenetic experiment, we further compared the change in average pairwise correlation before and after injection of the DREADD ligand. We only included those sites in this analysis which had at least 15 s behavior for each of the two compared conditions.

We defined latency to activation on locomotion onset (**Figure S1**) for a neuron or axon as the time after onset when the calcium activity, averaged across onsets, first was 2 standard deviations above baseline, and remained above this threshold thereafter for at least 1 s. Neurons that did not reach threshold within the analysis window −2 s to +3 s and were not significantly responsive to locomotion onset (paired two-sample t-test over onsets, $p < 0.05$, between baseline −1 s to −0.5 s and response +0.5 s to +1.5 s), were not included in the analysis.

Response latency to grating stimuli (**Figure 7**) was defined for a neuron as the time after onset when the calcium activity, averaged across onsets, first was 2 standard deviations above baseline, and remained above this threshold for at least 1/3 s. Neurons that did not reach threshold within the analysis window of 0 s to +2 s (equal to the duration of grating presentation) were not included in the analysis.

Statistical Analysis

All statistical information for the tests performed in the manuscript is provided in **Table S1**. Unless stated otherwise, the shading indicates the standard error of the mean across axons or neurons. For analysis where the experimental unit was axon, neuron, or pair of neurons, we used hierarchical bootstrap (Saravanan et al., 2020) for statistical testing due to the nested nature (axons/neurons and mice) of the data. Briefly, we first resampled the data (with replacement) at the level of imaging sites, and then, from the selected sites, resampled for axons (or neurons or neuron pairs). We then computed the mean of this bootstrap sample and repeated this 10 000 times (or 1000 times when comparing response traces in **Figures 4 and S6**) to generate a bootstrap distribution of the mean estimate. For paired tests, the p-value was defined as the proportion of bootstrap samples higher (or lower, depending on the hypothesis) than zero. For unpaired tests, the distribution of the mean for the two variables were compared as the proportion of values higher (or lower, depending on the hypothesis). For analysis where the experimental unit was imaging site, we first tested for normality using Kolmogorov-Smirnov test at a significance level of 5%. For datasets that did not pass the test for normality, the medians were compared with Wilcoxon rank-sum test or signed rank test, as applicable. Otherwise, the means were compared using paired or unpaired t-test, as applicable.

Supplemental tables

Figure panel	Value compared	Mean 1	SD 1	Mean 2	SD 2	Test	P-value	N (ROIs)	N (Sites)	N (Mice)
1K	Fraction of responsive cholinergic axons responsive to locomotion onsets *vs* grating onsets	0.523	0.220	0.063	0.075	t-test	$<10^{-5}$	-	**25**	14
	Fraction of responsive cholinergic axons responsive to locomotion onsets *vs* mismatch onsets	0.523	0.220	0.062	0.051	t-test	$<10^{-5}$	-	**25**	14
	Fraction of responsive cholinergic axons responsive to locomotion onsets	0.523	0.220	-	-	t-test	$<10^{-5}$	-	**25**	14
	Fraction of responsive cholinergic axons responsive to grating onsets	0.063	0.075	-	-	t-test	0.40	-	**25**	14
	Fraction of responsive cholinergic axons responsive to mismatch onsets	0.062	0.051	-	-	t-test	0.25	-	**25**	14
2A	Locomotion velocity at locomotion bout onset *vs* offset	0.020	0.008	0.014	0.005	Hierarchical bootstrap	0	**5048**	**25**	14
2B	Cholinergic axon activity [% ΔF/F] at locomotion bout onset *vs* offset	1.47	2.03	1.39	1.80	Hierarchical bootstrap	0.22	**5048**	**25**	14
2C	Correlation between locomotion bout onset and offset for cholinergic axon activity *vs* locomotion velocity	0.554	0.215	0.135	0.258	t-test	$<10^{-5}$	-	**25**	14
2E	Average cholinergic axon activity [% ΔF/F] for low *vs* intermediate locomotion velocity	1.01	0.022	1.01	0.022	Hierarchical bootstrap	0.58	**5048, 3657**	**25, 17**	14, 11
	Average cholinergic axon activity [% ΔF/F] for intermediate *vs* high locomotion velocity	1.01	0.022	1.01	0.008	Hierarchical bootstrap	0.59	**3657, 1282**	**17, 7**	11, 5
	Average cholinergic axon activity [% ΔF/F] for low *vs* high locomotion velocity	1.01	0.022	1.01	0.008	Hierarchical bootstrap	0.70	**5048, 1282**	**25, 7**	14, 5
2F	Correlation of activity of cholinergic axons with raw *vs* binarized velocity	0.083	0.082	0.099	0.092	Hierarchical bootstrap	0	**5048**	**25**	14
3A	Correlation of average cholinergic axon activity with locomotion velocity in closed loop *vs* open loop	0.286	0.170	0.322	0.199	t-test	0.15	-	**25**	14
	Correlation of average cholinergic axon activity with locomotion velocity in dark *vs* grating	0.319	0.200	0.311	0.167	t-test	0.77	-	**25**	14
	Correlation of average cholinergic axon activity with locomotion velocity in closed loop *vs* dark	0.286	0.170	0.319	0.200	t-test	0.27	-	**25**	14
	Correlation of average cholinergic axon activity with locomotion velocity in open loop *vs* grating	0.322	0.199	0.311	0.167	t-test	0.75	-	**25**	14

Table S1.

Statistical information on all analysis.

For statistical comparisons we used paired or unpaired t-tests, or hierarchical bootstraps as indicated in the table below. The units (ROIs, sites, or mice) over which testing was done are boldfaced. For hierarchical bootstraps the two levels of units used are boldfaced.

	Correlation of average cholinergic axon activity with locomotion velocity in open loop *vs* dark	0.322	0.199	0.319	0.200	t-test	0.93	-	**25**	14
	Correlation of average cholinergic axon activity with locomotion velocity in closed loop *vs* grating	0.286	0.170	0.311	0.167	t-test	0.33	-	**25**	14
3B	Correlation of average cholinergic axon activity with pupil diameter in closed loop *vs* open loop	0.165	0.150	0.277	0.170	t-test	0.0001	-	**25**	14
	Correlation of average cholinergic axon activity with pupil diameter in dark *vs* grating	0.002	0.141	0.300	0.136	Unpaired t-test	0.0000	-	**21, 25**	13, 14
	Correlation of average cholinergic axon activity with pupil diameter in closed loop *vs* dark	0.165	0.150	0.002	0.141	Unpaired t-test	0.0005	-	**25, 21**	14, 13
	Correlation of average cholinergic axon activity with pupil diameter in open loop *vs* grating	0.277	0.170	0.300	0.136	t-test	0.61	-	**25**	14
	Correlation of average cholinergic axon activity with pupil diameter in open loop *vs* dark	0.277	0.170	0.002	0.141	Unpaired t-test	0.0000	-	**25, 21**	14, 13
	Correlation of average cholinergic axon activity with pupil diameter in closed loop *vs* grating	0.165	0.150	0.300	0.136	t-test	0.0028	-	**25**	14
3C	Correlation of pupil diameter with locomotion velocity in closed loop *vs* open loop	0.324	0.217	0.457	0.215	t-test	0.0001	-	**25**	14
	Correlation of pupil diameter with locomotion velocity in dark *vs* grating	0.060	0.232	0.435	0.239	Unpaired t-test	0.0000	-	**21, 25**	13, 14
	Correlation of pupil diameter with locomotion velocity in closed loop *vs* dark	0.324	0.217	0.060	0.232	Unpaired t-test	0.0003	-	**25, 21**	14, 13
	Correlation of pupil diameter with locomotion velocity in open loop *vs* grating	0.457	0.215	0.435	0.239	t-test	0.70	-	**25**	14
	Correlation of pupil diameter with locomotion velocity in open loop *vs* dark	0.457	0.215	0.060	0.232	Unpaired t-test	0.0000	-	**25, 21**	14, 13
	Correlation of pupil diameter with locomotion velocity in closed loop *vs* grating	0.324	0.217	0.435	0.239	t-test	0.045	-	**25**	14
4A	Grating response difference in layer 2/3 neurons [% ΔF/F] while locomoting *vs* not locomoting	-0.12	10.66	-1.97	6.78	Hierarchical bootstrap	0	**6529**	**21**	14
4B	Grating response difference in layer 5 neurons [% ΔF/F] while locomoting *vs* not locomoting	3.13	8.10	0.88	5.50	Hierarchical bootstrap	0	**6798**	**25**	14
4C	Grating response difference in layer 2/3 neurons [% ΔF/F] on optogenetic stimulation *vs* no stimulation while not locomoting	-2.43	8.10	-2.44	7.44	Hierarchical bootstrap	0.46	**3992**	**13**	13
4D	Grating response difference in layer 5 neurons [% ΔF/F] on optogenetic stimulation *vs* no stimulation while not locomoting	1.21	6.05	0.62	6.06	Hierarchical bootstrap	0.0060	**4715**	**16**	13
4E	Mismatch response difference in layer 2/3 neurons [% ΔF/F] on optogenetic stimulation vs no stimulation	2.00	10.14	2.25	8.36	Hierarchical bootstrap	0.66	**2506**	**9**	9
4F	Mismatch response difference in layer 5 neurons [% ΔF/F] on optogenetic stimulation *vs* no stimulation	2.72	7.26	1.77	5.30	Hierarchical bootstrap	0.028	**2801**	**9**	6

Table S1. (continued)

4G	Locomotion onset response difference in closed loop in layer 2/3 neurons [% ΔF/F] on optogenetic stimulation *vs* no stimulation	1.66	9.36	1.23	5.76	Hierarchical bootstrap	0.13	**2747**	**10**	10
4H	Locomotion onset response difference in closed loop in layer 5 neurons [% ΔF/F] on optogenetic stimulation *vs* no stimulation	2.63	5.54	1.86	4.26	Hierarchical bootstrap	0	**3623**	**11**	8
5A	Mean response in layer 2/3 neurons [% ΔF/F] on locomotion onset *vs* zero	1.82	7.37	-	-	Hierarchical bootstrap	0	**6154**	**20**	14
5B	Mean response in layer 5 neurons [% ΔF/F] on locomotion onset *vs* zero	2.00	4.28	-	-	Hierarchical bootstrap	0	**6032**	**22**	12
5C	Mean response in layer 2/3 neurons [% ΔF/F] to optogenetic stimulation of ChAT axons *vs* zero	-0.07	6.63	-	-	Hierarchical bootstrap	0.62	**6154**	**20**	14
5D	Mean response in layer 5 neurons [% ΔF/F] on optogenetic stimulation of ChAT axons *vs* zero	-0.16	3.21	-	-	Hierarchical bootstrap	0.86	**6032**	**22**	13
6E	Difference in average pairwise correlation of layer 2/3 neurons while locomoting *vs* not locomoting	0.035	0.020	0.038	0.021	Hierarchical bootstrap	0.045	**7826**	**25**	15
	Difference in average pairwise correlation of layer 2/3 neurons on optogenetic stimulation *vs* no stimulation while not locomoting	0.021	0.018	0.029	0.022	Hierarchical bootstrap	0	**1688**	**4**	4
6F	Difference in average pairwise correlation of layer 5 neurons while locomoting *vs* not locomoting	0.030	0.017	0.036	0.017	Hierarchical bootstrap	$<10^{-3}$	**7132**	**26**	14
	Difference in average pairwise correlation of layer 5 neurons on optogenetic stimulation *vs* no stimulation while not locomoting	0.009	0.010	0.014	0.009	Hierarchical bootstrap	0.0017	**100**	**4**	4
6G	Layer 2/3 neuron difference in the change in average pairwise correlation on locomotion following ligand injection for DREADD activation *vs* inhibition	-0.0005	$<10^{-3}$	-0.002	$<10^{-3}$	Hierarchical bootstrap	0.32	**2429, 3103**	**7, 10**	7, 9
6H	Layer 5 neuron difference in the change in average pairwise correlation on locomotion following ligand injection for DREADD activation *vs* inhibition	-0.003	$<10^{-3}$	0.007	$<10^{-3}$	Hierarchical bootstrap	0.032	**1651, 1762**	**7, 7**	7, 7
7A	Latency to grating response onset in layer 2/3 neurons [ms] while locomoting *vs* not locomoting	596	470	632	451	Hierarchical bootstrap	0.86	**1481**	**24**	15
	Latency to grating response onset in layer 2/3 neurons [ms] on optogenetic stimulation *vs* no stimulation while not locomoting	656	427	659	444	Hierarchical bootstrap	0.54	**1503**	**15**	15
7B	Latency to grating response onset in layer 5 neurons [ms] while locomoting *vs* not locomoting	658	413	771	417	Hierarchical bootstrap	0.0037	**938**	**25**	14
	Latency to grating response onset in layer 5 neurons [ms] on optogenetic stimulation *vs* no stimulation while not locomoting	709	407	793	413	Hierarchical bootstrap	0.0046	**783**	**16**	13
S1D	Latency to response on locomotion onset [ms] for cholinergic axons *vs* layer 2/3 neurons	477	457	366	614	Hierarchical bootstrap	0.040	**1182, 1166**	**23, 25**	12, 15
	Latency to response on locomotion onset [ms] for cholinergic axons *vs* layer 5 neurons	477	457	635	503	Hierarchical bootstrap	0.014	**1182, 1299**	**23, 26**	12, 14

Table S1. (continued)

	Latency to response on locomotion onset [ms] for layer 2/3 neurons *vs* layer 5 neurons	366	614	635	503	Hierarchical bootstrap	0	**1166, 1299**	**25, 26**	15, 14
S2G	Correlation of cholinergic axon population activity vector between bout onset and during the bout for actual *vs* random triggers	0.735	0.187	0.007	0.088	t-test	$<10^{-5}$	-	**25**	14
	Correlation of cholinergic axon population activity vector between during the bout and at bout onset for actual *vs* random triggers	0.759	0.194	0.036	0.120	t-test	$<10^{-5}$	-	**25**	14
	Correlation of cholinergic axon population activity vector between bout onset and offset for actual *vs* random triggers	0.721	0.196	0.012	0.103	t-test	$<10^{-5}$	-	**25**	14
S2H	Average GRAB-ACh activity [% ΔF/F] in visual cortex during low *vs* high velocity	1.3	3.4	0.22	3.9	Hierarchical bootstrap	0.7	**178, 132**	**8,6**	8,6
S4A	Variability in pupil diameter [SD] in closed loop *vs* open loop	21.32	8.47	18.68	5.48	t-test	0.15	-	**25**	14
	Variability in pupil diameter [SD] in dark *vs* grating	25.52	17.45	16.54	7.16	Unpaired t-test	0.023	-	**21, 25**	13, 14
	Variability in pupil diameter [SD] in closed loop *vs* dark	21.32	8.47	25.52	17.45	Unpaired t-test	0.29	-	**25, 21**	14, 13
	Variability in pupil diameter [SD] in open loop *vs* grating	18.68	5.48	16.54	7.16	t-test	0.10	-	**25**	14
	Variability in pupil diameter [SD] in open loop *vs* dark	18.68	5.48	25.52	17.45	Unpaired t-test	0.070	-	**25, 21**	14, 13
	Variability in pupil diameter [SD] in closed loop *vs* grating	21.32	8.47	16.54	7.16	t-test	0.041	-	**25**	14
S4B	Correlation of average cholinergic axon activity with locomotion velocity *vs* facial movement in closed loop	0.286	0.170	0.095	0.172	t-test	$<10^{-4}$	-	**25**	14
	Correlation of average cholinergic axon activity with locomotion velocity *vs* facial movement in open loop	0.322	0.199	0.148	0.195	t-test	0.0001	-	**25**	14
	Correlation of average cholinergic axon activity with locomotion velocity *vs* facial movement in dark	0.319	0.200	0.090	0.224	t-test	$<10^{-4}$	-	**25**	14
	Correlation of average cholinergic axon activity with locomotion velocity *vs* facial movement in grating condition	0.311	0.167	0.130	0.214	t-test	0.0001	-	**25**	14
S5A	Mice locomotion velocity [cm/s] on optogenetic stimulation of cholinergic axons, before *vs* after	2.53	3.09	2.4	3.09	Hierarchical bootstrap	0.81	-	**51, 51**	15, 15
S5B	Average locomotion velocity [cm/s], before *vs* upon optogenetic stimulation of cholinergic axons in visual cortex	2.53	3.09	2.4	3.09	Hierarchical bootstrap	0.81	-	**51, 51**	15, 15
S6F	Change in average pairwise correlation of layer 2/3 neuron on control stimulation *vs* no stimulation while not locomoting	0.025	0.030	0.025	0.022	Hierarchical bootstrap	0.46	**1047**	**3**	3
	Change in average pairwise correlation of layer 5 neurons on control stimulation *vs* no stimulation while not locomoting	0.017	0.021	0.012	0.006	Hierarchical bootstrap	0.18	**88**	**3**	3
S7A	Mean response in layer 2/3 neurons [% ΔF/F] to grating onset (preferred + π/4 Ori) stationary *vs* locomotion	-3.10	9.36	-0.30	9.95	Hierarchical bootstrap	0	**2396, 2500**	**13, 13**	13, 13

Table S1. (continued)

	Mean response in layer 2/3 neurons [% ΔF/F] to grating onset (preferred Ori) stationary *vs* locomotion	-1.50	12.87	1.80	18.57	Hierarchical bootstrap	0	**3908, 3992**	**13, 13**	13, 13
	Mean response in layer 2/3 neurons [% ΔF/F] to grating onset (preferred - π/4 Ori) stationary *vs* locomotion	-2.67	9.84	-0.84	11.83	Hierarchical bootstrap	0.002	**2729, 2729**	**13, 13**	13, 13
	Mean response in layer 2/3 neurons [% ΔF/F] to grating onset (preferred + π/2 Ori) stationary *vs* locomotion	-2.64	9.04	-0.92	13.97	Hierarchical bootstrap	0.009	**2519, 2572**	**13, 13**	13, 13
	Mean response in layer 2/3 neurons [% ΔF/F] to grating onset (preferred + π/4 Ori) stationary *vs* (stationary + opto)	-3.10	9.36	-2.50	6.95	Hierarchical bootstrap	0.08	**2396, 2500**	**13, 13**	13, 13
	Mean response in layer 2/3 neurons [% ΔF/F] to grating onset (preferred Ori) stationary *vs* (stationary + opto)	-1.50	12.87	-1.33	10.54	Hierarchical bootstrap	0.27	**3908, 3992**	**13, 13**	13, 13
	Mean response in layer 2/3 neurons [% ΔF/F] to grating onset (preferred - π/4 Ori) stationary *vs* (stationary + opto)	-2.67	9.84	-2.59	7.61	Hierarchical bootstrap	0.42	**2729, 2729**	**13, 13**	13, 13
	Mean response in layer 2/3 neurons [% ΔF/F] to grating onset (preferred + π/2 Ori) stationary *vs* (stationary + opto)	-2.64	9.04	-2.22	8.33	Hierarchical bootstrap	0.32	**2519, 2572**	**13, 13**	13, 13
S7B	Mean response in layer 5 neurons [% ΔF/F] to grating onset (preferred + π/4 Ori) stationary *vs* locomotion	-0.26	10.40	2.01	10.72	Hierarchical bootstrap	10^{-4}	**3448, 3520**	**16, 16**	13, 13
	Mean response in layer 5 neurons [% ΔF/F] to grating onset (preferred Ori) stationary *vs* locomotion	0.28	11.76	4.49	15.16	Hierarchical bootstrap	0	**4670, 4715**	**16, 16**	13, 13
	Mean response in layer 5 neurons [% ΔF/F] to grating onset (preferred - π/4 Ori) stationary *vs* locomotion	-0.28	9.58	2.77	9.74	Hierarchical bootstrap	0	**3518, 3614**	**16, 16**	13, 13
	Mean response in layer 5 neurons [% ΔF/F] to grating onset (preferred + π/2 Ori) stationary *vs* locomotion	-0.83	8.85	2.33	9.66	Hierarchical bootstrap	0	**3642, 3642**	**16, 16**	13, 13
	Mean response in layer 5 neurons [% ΔF/F] to grating onset (preferred + π/4 Ori) stationary *vs* (stationary + opto)	-0.26	10.40	-0.10	7.18	Hierarchical bootstrap	0.30	**3448, 3520**	**16, 16**	13,
	Mean response in layer 5 neurons [% ΔF/F] to grating onset (preferred Ori) stationary *vs* (stationary + opto)	0.28	11.76	1.37	9.62	Hierarchical bootstrap	0	**4670, 4715**	**16, 16**	13, 13
	Mean response in layer 5 neurons [% ΔF/F] to grating onset (preferred - π/4 Ori) stationary *vs* (stationary + opto)	-0.28	9.58	0.14	7.23	Hierarchical bootstrap	0.13	**3518, 3614**	**16, 16**	13, 13
	Mean response in layer 5 neurons [% ΔF/F] to grating onset (preferred + π/2 Ori) stationary *vs* (stationary + opto)	-0.83	8.85	-0.53	6.02	Hierarchical bootstrap	0.22	**3642, 3642**	**16, 16**	13, 13
S10 B	Locomotion velocity before *vs* after DREADD activation	0.022	0.005	0.028	0.005	t-test	$<10^{-3}$	-	**14**	7
	Locomotion velocity before *vs* after DREADD inhibition	0.017	0.004	0.016	0.005	t-test	0.46	-	**17**	9
S10 D	Time spent locomoting before *vs* after DREADD activation	0.683	0.143	0.699	0.154	t-test	0.64	-	**14**	7
	Time spent locomoting before *vs* after DREADD inhibition	0.572	0.156	0.360	0.164	t-test	$<10^{-5}$	-	**17**	9

Table S1. (continued)

S10E	Total distance run before *vs* after DREADD activation	5.086	1.964	6.511	2.457	t-test	0.0067	-	**14**	7
	Total distance run before *vs* after DREADD inhibition	3.314	1.713	2.144	1.413	t-test	$<10^{-4}$	-	**17**	9
	Change in total distance run on DREADD activation *vs* inhibition	1.425	1.657	-1.170	0.913	Unpaired t-test	$<10^{-5}$	-	**14, 17**	7, 9
S11 A	Change in average pairwise correlation on locomotion in layer 2/3 neurons in DREADD activation group pre-CNO *vs* zero	-0.010	0.019	-	-	Hierarchical bootstrap	0	**2429**	**7**	**7**
	Change in average pairwise correlation on locomotion in layer 2/3 neurons in DREADD activation group post-CNO *vs* zero	-0.010	0.019	-	-	Hierarchical bootstrap	10^{-4}	**2429**	**7**	**7**
	Change in average pairwise correlation on locomotion in layer 2/3 neurons in DREADD inhibition group pre-CNO *vs* zero	-0.004	0.019	-	-	Hierarchical bootstrap	0.01	**3103**	**10**	9
	Change in average pairwise correlation on locomotion in layer 2/3 neurons in DREADD inhibition group post-CNO *vs* zero	-0.006	0.020	-	-	Hierarchical bootstrap	0.02	**3103**	**10**	9
S11 B	Change in average pairwise correlation on locomotion in layer 5 neurons in DREADD activation group pre-CNO *vs* zero	-0.008	0.016	-	-	Hierarchical bootstrap	0	**1651**	**7**	**7**
	Change in average pairwise correlation on locomotion in layer 5 neurons in DREADD activation group post-CNO *vs* zero	-0.011	0.019	-	-	Hierarchical bootstrap	0.003	**1651**	**7**	**7**
	Change in average pairwise correlation on locomotion in layer 5 neurons in DREADD inhibition group pre-CNO *vs* zero	-0.010	0.020	-	-	Hierarchical bootstrap	0.001	**1762**	**7**	**7**
	Change in average pairwise correlation on locomotion in layer 5 neurons in DREADD inhibition group post-CNO *vs* zero	-0.002	0.016	-	-	Hierarchical bootstrap	0.23	**1762**	**7**	**7**

Table S1. (continued)

Genotype	Virus	Site of injection	Nbr. Mice	Nbr. ROIs	Figures
ChAT-IRES-Cre	AAV2/5-hSyn1-FLEx-axon-GCaMP6s	Basal forebrain – MS/vDB/hDB	12	4451	Figures 1, 2, 3, S1, S2G, S3, S4
ChAT-IRES-Cre	AAV PHP.eB-Ef1α-DIO-GCaMP6s	Basal forebrain – MS/vDB/hDB	2	597	Figures 1, 2, 3, S1, S2G, S3, S4
ChAT-IRES-Cre	AAV2/1-hSyn-DIO-ChrimsonR-tdTomato	Basal forebrain – MS/vDB/hDB	15	15 103	Figures 4, 5, 6A-6F, 7, S1, S6D and S6E, S6F, S9
	AAV2/1-Ef1α-GCaMP6f-WPRE	Primary visual cortex			
ChAT-IRES-Cre	AAV2/1-Ef1α-DIO-hM3D(Gq)-mCherry	Basal forebrain – MS/vDB/hDB	7	4080	Figures 6G-6H, S10
	AAV2/1-Ef1α-GCaMP6f-WPRE	Primary visual cortex			
ChAT-IRES-Cre	AAV2/1-Ef1α-DIO-hM4D(Gi)-mCherry	Basal forebrain – MS/vDB/hDB	9	4865	Figures 6G-6H, S10
	AAV2/1-Ef1α-GCaMP6f-WPRE	Primary visual cortex			
ChAT-IRES-Cre	AAV2/9-hSyn-GRAB-ACh3.0	Primary visual cortex	8	609	Figures S2A-S2C, S2H
ChAT-IRES-Cre	AAV2/1-Ef1α-DIO-tdTomato-WPRE	Basal forebrain – MS/vDB/hDB	5	2409	Figures S6A-S6C
	AAV2/1-Ef1α-GCaMP6f-WPRE	Primary visual cortex			
ChAT-IRES-Cre	AAV2/1-Ef1α-eGFP-WPRE	Primary visual cortex	6	2640	Figures S2D-S2F

Table S2.

Number of mice in different experimental groups

Supplementary figures

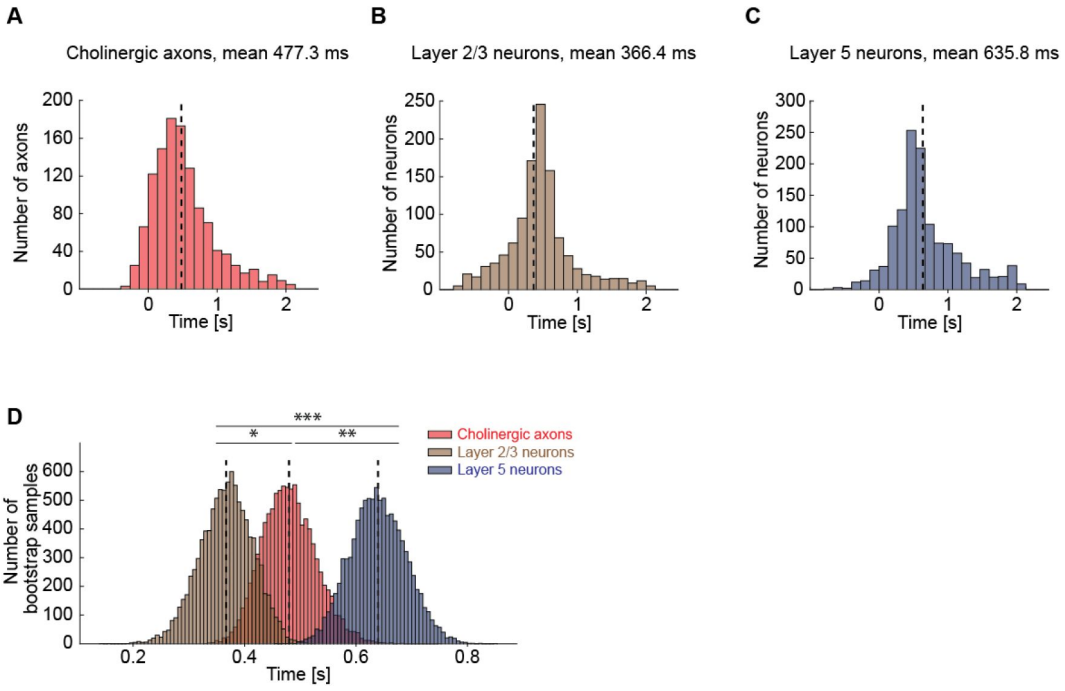

Figure S1.

Cholinergic axons in visual cortex were activated after layer 2/3 but before layer 5 visual cortex neurons. Related to Figure 1 .|

(**A**) Distribution of time to first significant response after locomotion onset for cholinergic axons in visual cortex. Axons without any response to locomotion onset are omitted.
(**B**) As in **A**, but for layer 2/3 neurons in visual cortex.
(**C**) As in **A**, but for layer 5 neurons in visual cortex.
(**D**) Nested bootstrap resampling of the distributions shown in **A-C**. Here and elsewhere, n.s.: not significant; *: p<0.05; **: p<0.01; ***: p<0.001; see **Table S1** for all statistical information.

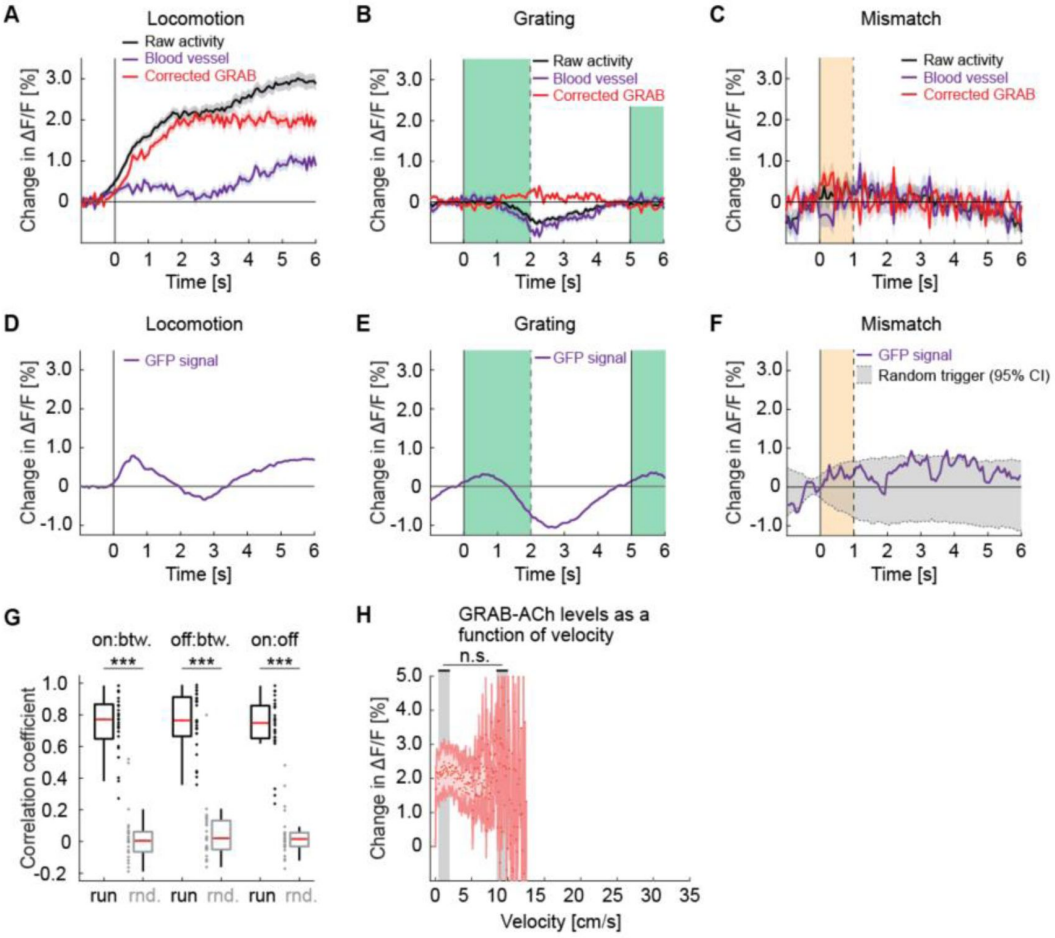

Figure S2.

Responses of GRAB-ACh3.0 in visual cortex are similar to the calcium responses in cholinergic axons. Related to Figure 2.

(**A**) Average change in GRAB-ACh3.0 fluorescence during locomotion onset. We used the fluorescence change measured in blood vessels (purple) to estimate hemodynamic occlusion and subtracted this from the raw activity (black) to generate a corrected response (red). Shading marks SEM.
(**B**) As in **A**, but for the GRAB-ACh3.0 response to grating onsets. The green shading marks the duration of the grating stimulus.
(**C**) As in **A**, but for the GRAB-ACh3.0 response to visuomotor mismatch. The orange shading marks the duration of the visuomotor mismatch.
(**D**) To estimate hemodynamic occlusion effects while two-photon imaging, we measured fluorescence changes on locomotion onset in layer 2/3 neurons in visual cortex that express GFP.
(**E**) As in **D**, but for responses to grating onsets.
(**F**) As in **D**, but for responses to visuomotor mismatch.
(**G**) The correlation coefficient between the population activity vectors during locomotion onset (on), offset (off), and during locomotion bout (btw), compared to shuffle (rnd.) controls. Here and elsewhere, n.s.: not significant; *: p<0.05; **: p<0.01; ***: p<0.001; see **Table S1** for all statistical information.
(**H**) GRAB-ACh3.0 fluorescence as a function of locomotion velocity. Shown are the mean acetylcholine level in each bin, corrected for hemodynamics. Shading marks SEM. We found no evidence of a difference in acetylcholine level between low and high locomotion velocities (indicated by gray shading). Note, the x-axis range is matched to that in **Figure 2E**. Because we had overall less data in these GRAB experiments, reliable estimates of mean acetylcholine levels were not possible for locomotion velocities above approximately 13 cm/s.

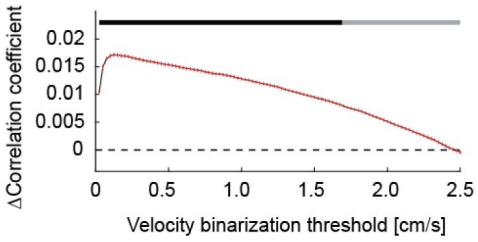

Figure S3.

Cholinergic axon activity correlated better with a binarized locomotion vector than with the unfiltered locomotion vector over a large range of binarization thresholds. Related to Figure 2.

The correlation between activity of cholinergic axons in visual cortex and locomotion velocity was higher when we used a binarized version of the locomotion velocity trace. This difference was present over a large range of thresholds. The black bar at the top of the plot indicates threshold values for which the correlation with binarized locomotion velocity was higher than that with raw locomotion velocity.

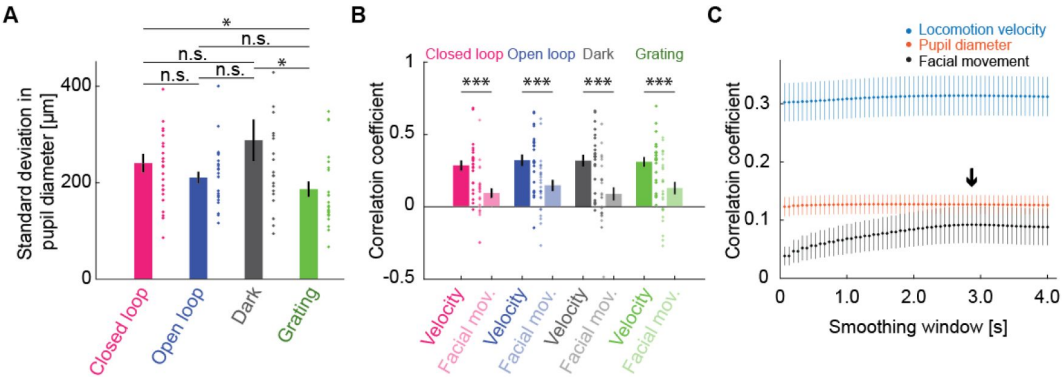

Figure S4.

Activity of cholinergic axons correlated better with locomotion velocity than with facial movement. Related to Figure 3.

(**A**) Standard deviation of pupil diameter as a function of visuomotor condition. Here and elsewhere, n.s.: not significant; *: $p < 0.05$; **: $p < 0.01$; ***: $p < 0.001$; see **Table S1** for all statistical information.
(**B**) Average correlation of activity of cholinergic axons in visual cortex with facial movements as a function of visuomotor condition, compared with the same activity correlation to locomotion velocity (same data as **Figure 3A**). Error bars indicate SEM. Individual data points are imaging sites.
(**C**) Average correlation of activity of cholinergic axons in visual cortex and locomotion velocity (blue), pupil diameter (red), or facial movement (black) as a function of smoothing window. The black arrow marks the smoothing window used for facial movements.

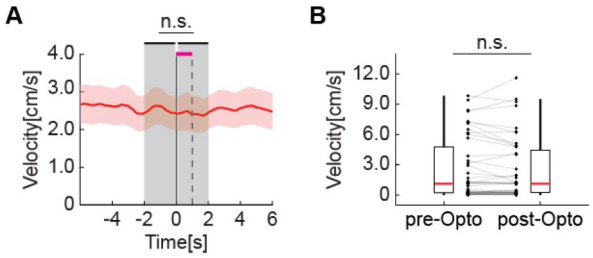

Figure S5.

Optogenetic stimulation of basal forebrain cholinergic axons in visual cortex did not change the locomotion velocity of the mice. Related to Figure 4.

(**A**) Locomotion velocity before, during, and after optogenetic stimulation of cholinergic axons. Shown are the mean (red line) and SEM (red shading) across imaging sites. Here and elsewhere, n.s.: not significant; *: p<0.05; **: p<0.01; ***: p<0.001; see **Table S1** for all statistical information.
(**B**) Average locomotion velocity before optogenetic stimulation (−2 s to 0 s) is indistinguishable from the locomotion velocity during and immediately after stimulation (0 s to 2 s; stimulation occurs from 0 s to 1 s). Each dot is an imaging site. Boxes show 25th and 75th percentile, red line is the median, and the whiskers extend to the most extreme datapoints not considered outliers.

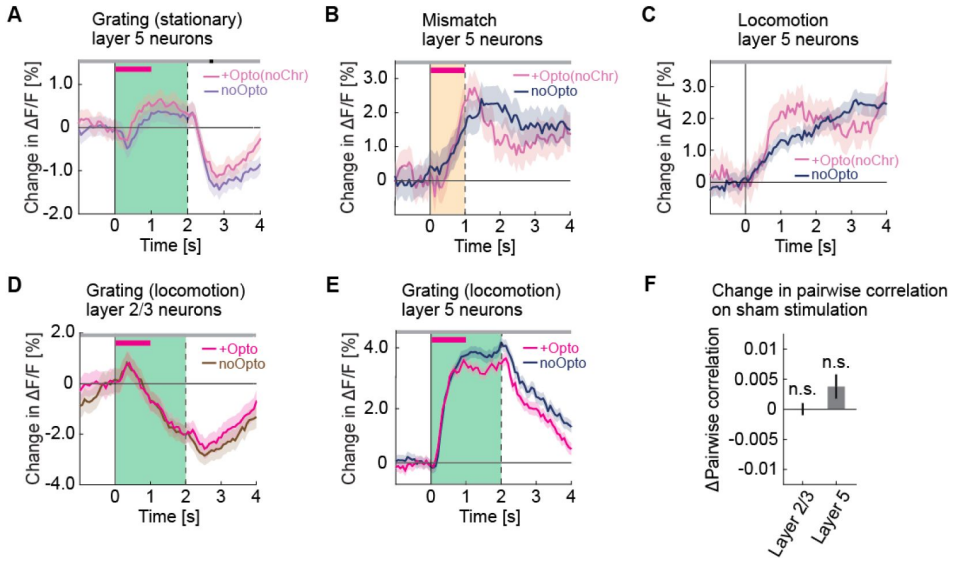

Figure S6.

Optogenetic activation did not increase grating responses during locomotion and had no effect in opsin-negative control mice. Related to Figures 4 and 6.

(**A**) Average calcium response of layer 5 neurons in visual cortex to full field drifting gratings (green shading) presented while the mice were stationary, without (pale blue) and with (pale pink) optogenetic stimulation in mice that did not express ChrimsonR in cholinergic axons. The duration of stimulation is marked by a pink bar.
(**B**) Average calcium response of layer 5 neurons in visual cortex to visuomotor mismatch (orange shading) without (blue) and with (pale pink) optogenetic light stimulation in mice that do not express ChrimsonR in cholinergic axons. The duration of stimulation light is marked by a pink bar.
(**C**) As in **B**, but for locomotion onset responses. Note, the locomotion onset threshold was relaxed to 0.025 cm/s to increase the number of onsets we could analyze.
(**D**) Average calcium response of layer 2/3 neurons in visual cortex to full field drifting gratings (green shading) presented while the mice were locomoting, without (brown) and with (pink) optogenetic stimulation of cholinergic axons in visual cortex. The duration of optogenetic stimulation is marked by a pink bar. The responses are compared bin-by-bin using a nested hierarchical bootstrap test. Here and in subsequent panels, bins with a significant difference ($p < 0.05$) are indicated by a black line above the plot; those with $p > 0.05$ are marked gray. Shading marks SEM.
(**E**) As in **D**, but for layer 5 neurons.
(**F**) Change in pairwise correlations in layer 2/3 neurons and in layer 5 neurons in visual cortex during sham stimulation while the mice were stationary. Here and elsewhere, n.s.: not significant; *: $p < 0.05$; **: $p < 0.01$; ***: $p < 0.001$; see **Table S1** for all statistical information.

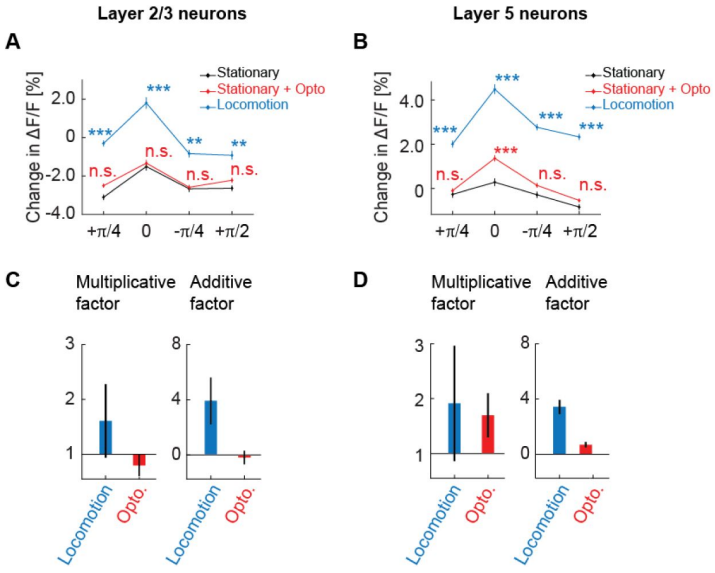

Figure S7.

Cholinergic stimulation primarily has a multiplicative influence on the orientation tuning curve of layer 5 neurons. Related to Figure 4.

(**A**) Average calcium response of layer 2/3 neurons in visual cortex to different orientations of full field drifting gratings while mice were stationary (black), on optogenetic stimulation of cholinergic axons while mice were stationary (red), and while mice were locomoting (blue). Here and elsewhere, n.s.: not significant; *: $p < 0.05$; **: $p < 0.01$; ***: $p < 0.001$; see **Table S1** for all statistical information.
(**B**) As in **A**, but for layer 5 neurons in visual cortex.
(**C**) Muliplicative factor (a) and additive factor (b) of a linear fit of the form y = ax +b, for the scaling of the orientation tuning curve in layer 2/3 induced by locomotion and optogenetic stimulation of cholinergic axons. Error bars indicate the standard error of the coefficients.
(**D**) Same as in **C**, but for layer 5 neurons in visual cortex.

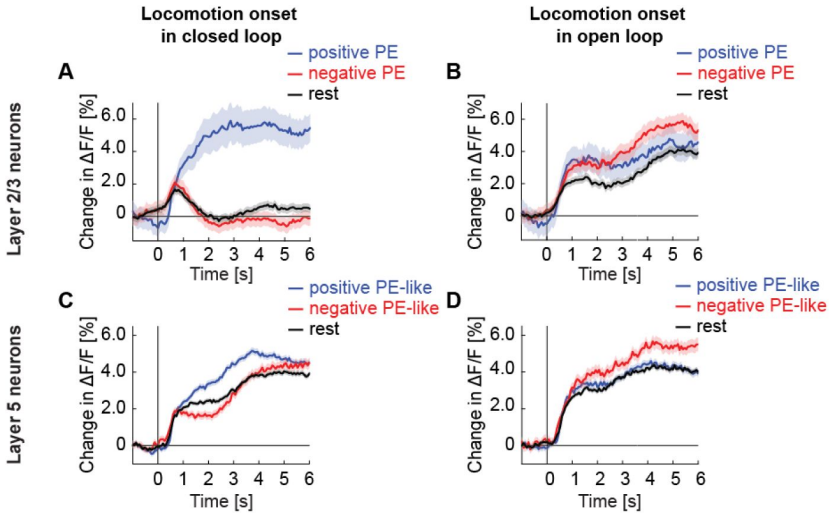

Figure S8.

Locomotion onset responses are suppressed by closed loop visual feedback in layer 2/3, but not layer 5. Related to Figures 4G and 4H.

(**A**) Average calcium response of layer 2/3 neurons in visual cortex to locomotion onset in closed loop, with neurons split into positive prediction error (PE) neurons (blue), negative PE neurons (red), and the rest of the population (black). We defined the top 30% responders to grating stimuli as positive PE neurons, the top 30% responders to visuomotor mismatch as negative PE neurons, and the remaining 60% of the neurons along with any neurons that responded to both gratings and mismatch as rest.
(**B**) As in **A**, but during open loop.
(**C**) As in **A**, but for layer 5 neurons.
(**D**) As in **A**, but for layer 5 neurons in open loop.

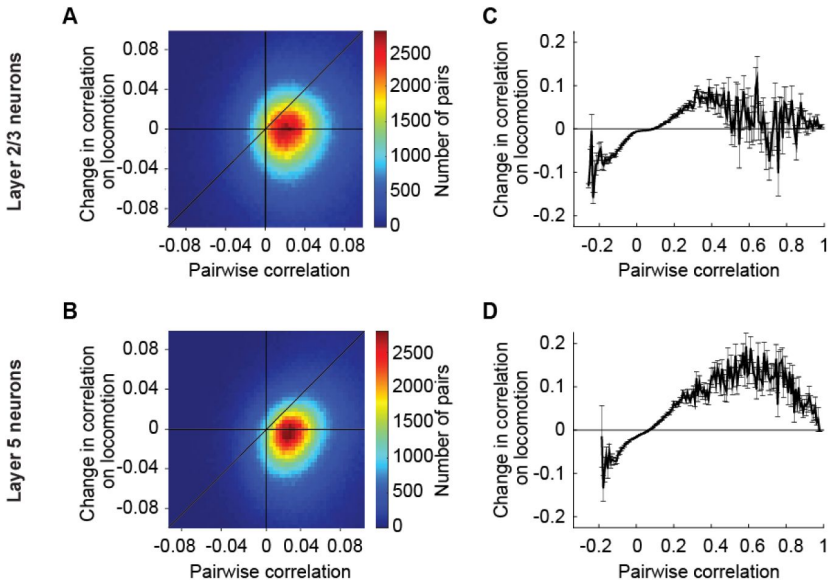

Figure S9.

Locomotion increases the correlation between those layer 5 neurons in visual cortex that on average have a higher correlation. Related to Figure 6.

(**A**) Change in the pairwise correlation between pairs of layer 2/3 neurons in visual cortex on locomotion and their average correlation over the entire imaging session.
(**B**) As in **A**, but for layer 5 neurons in visual cortex.
(**C**) Related to **A,** with all neuron pairs binned by their average correlation. Bars indicate SEM.
(**D**) As in **C,** but for layer 5 neurons in visual cortex.

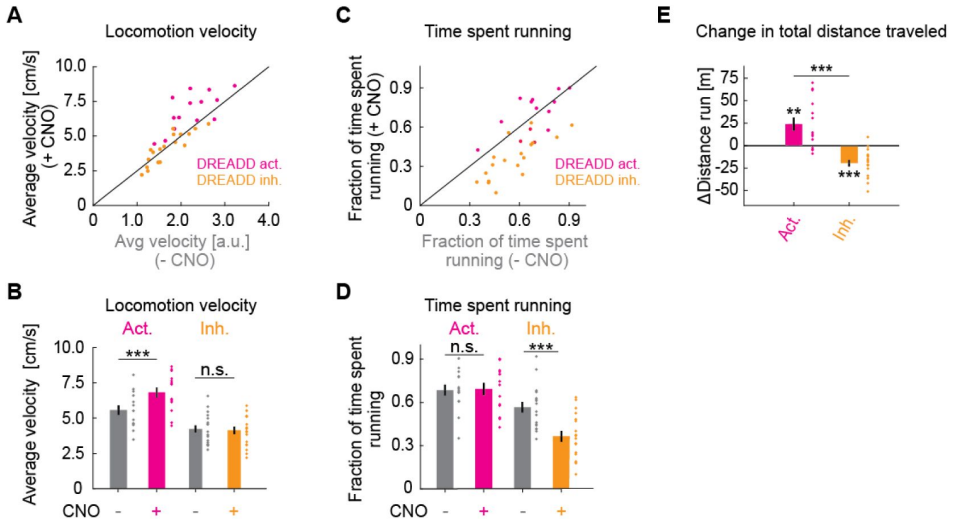

Figure S10.

Chemogenetic manipulation of basal forebrain cholinergic neurons affects locomotion behavior of mice. Related to Figure 6.

(**A**) Average locomotion velocity before and after administration of CNO in ChAT-Cre mice that expressed a DREADD activator (pink) or a DREADD inhibitor (orange) in basal forebrain. Each dot is an experimental session.
(**B**) Quantification of the data shown in **A**. Here and elsewhere, n.s.: not significant; *: $p < 0.05$; **: $p < 0.01$; ***: $p < 0.001$; see **Table S1** for all statistical information.
(**C**) As in **A**, but for fraction of time spent running.
(**D**) Quantification of the data shown in **C**.
(**E**) CNO induced change in the total distance traveled.

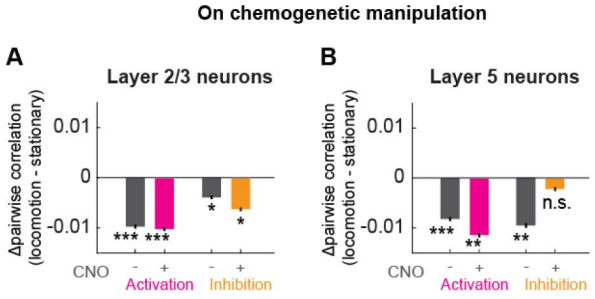

Figure S11.

Change in locomotion-related decorrelation upon chemogenetic manipulation of basal forebrain cholinergic neurons. Related to Figure 6.

(**A**) Average change in pairwise correlations of layer 2/3 neurons of visual cortex during locomotion in the group of mice before (gray, left) and after (pink) DREADD activation, and in the group before (gray, right) and after (orange) DREADD inhibition of basal forebrain cholinergic neurons. Here and elsewhere, n.s.: not significant; *: $p < 0.05$; **: $p < 0.01$; ***: $p < 0.001$; see **Table S1** for all statistical information. Note, the differences in pre-CNO locomotion driven decorrelation between the different groups of mice complicate the direct comparison of the DREADD effects. To ease this comparison, we represented the same data in **Figure 6G and 6H** as a difference to pre-CNO levels.
(**B**) As in **A**, but for layer 5 neurons of visual cortex.

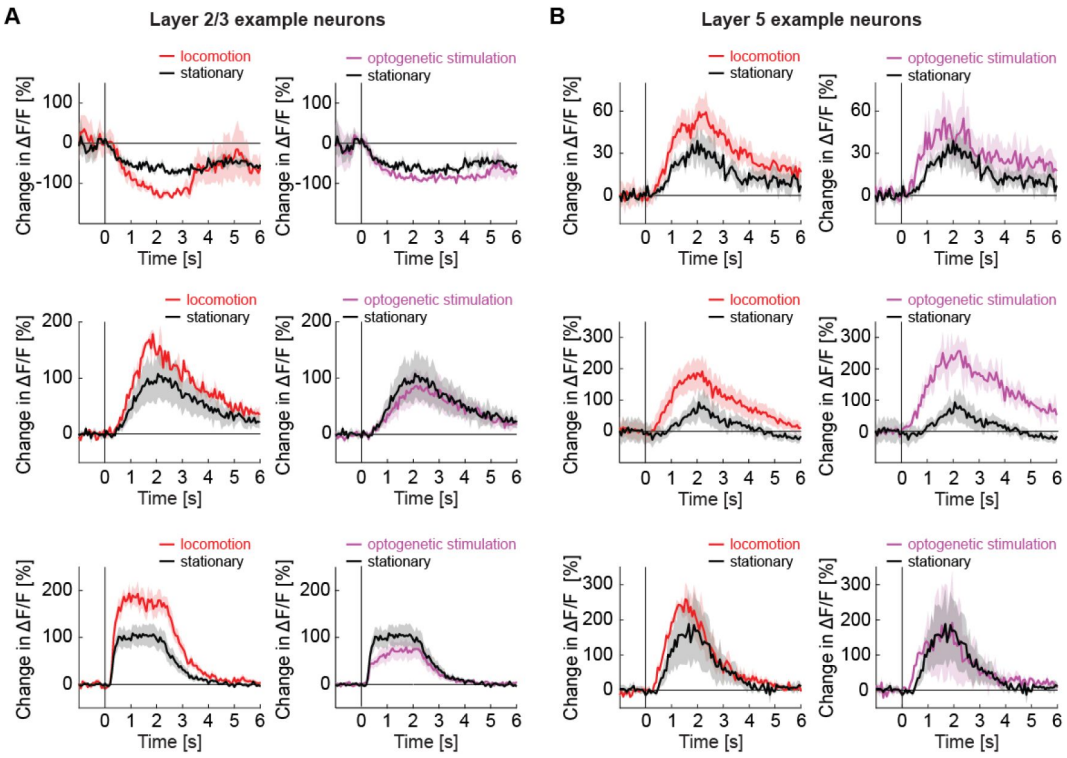

Figure S12.

Locomotion and optogenetic stimulation of basal forebrain cholinergic axons decreased the latency of response to a visual stimulus in layer 5 neurons but not in layer 2/3 neurons. Related to Figure 7.

(**A**) Three example layer 2/3 neurons from visual cortex with the average response to grating stimuli in responsive trials while the mouse is stationary (black), locomoting (red), or on optogenetic stimulation of cholinergic axons in visual cortex (purple). (**B**) As in **A**, but for three example layer 5 neurons.

Acknowledgements

We thank all the members of the Keller lab for discussion and support. This project has received funding from the Swiss National Science Foundation (GBK), the Novartis Research Foundation (GBK), and the European Research Council (ERC) under the European Union's Horizon 2020 research and innovation programme (grant agreement No 865617) (GBK).

Author contributions

BY designed and performed the experiments and analyzed the data. All authors wrote the manuscript.

Declaration of interests

The authors declare no competing financial interests.

References

Alitto H.J., Dan Y (2012) **Cell-type-specific modulation of neocortical activity by basal forebrain input** *Front. Syst. Neurosci* https://doi.org/10.3389/fnsys.2012.00079

Attinger A., Wang B., Keller G.B., Attinger A., Wang B., Keller G.B (2017) **Visuomotor coupling shapes the functional development of mouse visual cortex** *Cell* **169**:1291–1302 https://doi.org/10.1016/j.cell.2017.05.023

Ayaz A., Saleem A.B., Schölvinck M.L., Carandini M (2013) **Locomotion Controls Spatial Integration in Mouse Visual Cortex** *Curr. Biol* **23**:890–894 https://doi.org/10.1016/J.CUB.2013.04.012

Aydın Ç., Couto J., Giugliano M., Farrow K., Bonin V (2018) **Locomotion modulates specific functional cell types in the mouse visual thalamus** *Nat. Commun* **9** https://doi.org/10.1038/s41467-018-06780-3

Bakin JS., Weinberger NM., Sharma J., Perea G., Petravicz J., Le C., Sur M (2012) **Induction of a physiological memory in the cerebral cortex by stimulation of the nucleus basalis** *PNAS* **93**:11219–11224 https://doi.org/10.1073/pnas.93.20.11219

Bear M.F., Singer W (1986) **Modulation of visual cortical plasticity by acetylcholine and noradrenaline** *Nature* **320**:172–176 https://doi.org/10.1038/320172a0

Broussard G.J., Liang Y., Fridman M., Unger E.K., Meng G., Xiao X., Ji N., Petreanu L., Tian L (2018) **In vivo measurement of afferent activity with axon-specific calcium imaging** *Nat. Neurosci* **21** https://doi.org/10.1038/s41593-018-0211-4

Chatfield P.O., Dempsey E.W. (1941) **Some effects of prostigmine and acetylcholine on cortical potentials**

Chen N., Sugihara H., Sur M (2015) **An acetylcholine-activated microcircuit drives temporal dynamics of cortical activity** *Nat. Neurosci* **18**:892–902 https://doi.org/10.1038/nn.4002

Colangelo C., Shichkova P., Keller D., Markram H., Ramaswamy S (2019) **Cellular, synaptic and network effects of acetylcholine in the neocortex** *Front. Neural Circuits* **13** https://doi.org/10.3389/fncir.2019.00024

Collins L., Francis J., Emanuel B., McCormick D.A (2023) **Cholinergic and noradrenergic axonal activity contains a behavioral-state signal that is coordinated across the dorsal cortex** *eLife* **12** https://doi.org/10.7554/eLife.81826

Dadarlat M.C., Stryker M.P (2017) **Locomotion enhances neural encoding of visual stimuli in mouse V1** *J. Neurosci* **37**:3764–3775 https://doi.org/10.1523/JNEUROSCI.2728-16.2017

Davies P., Maloney A.J (1976) **Selective loss of central cholinergic neurons in Alzheimer's disease** *Lancet Lond. Engl* **2** https://doi.org/10.1016/s0140-6736(76)91936-x

Dombeck D.A., Khabbaz A.N., Collman F., Adelman T.L., Tank D.W (2007) **Imaging large-scale neural activity with cellular resolution in awake, mobile mice** *Neuron* **56**:43–57 https://doi.org/10.1016/j.neuron.2007.08.003

Eggermann E., Kremer Y., Crochet S., Petersen C.C.H (2014) **Cholinergic Signals in Mouse Barrel Cortex during Active Whisker Sensing** *Cell Rep* **9**:1654–1660 https://doi.org/10.1016/j.celrep.2014.11.005

Ego-Stengel V., Shulz D.E., Haidarliu S., Sosnik R., Ahissar E (2001) **Acetylcholine-Dependent Induction and Expression of Functional Plasticity in the Barrel Cortex of the Adult Rat** *J. Neurophysiol* **86**:422–437 https://doi.org/10.1152/jn.2001.86.1.422

Erisken S., Vaiceliunaite A., Jurjut O., Fiorini M., Katzner S., Busse L (2014) **Effects of Locomotion Extend throughout the Mouse Early Visual System** *Curr. Biol* **24**:2899–2907 https://doi.org/10.1016/j.cub.2014.10.045

Forster F.M., McCarter R.H (1946) **The effects of local applications of acetylcholine to the acoustic cortex** *J. Neuropathol. Exp. Neurol* **5**:24–28 https://doi.org/10.1097/00005072-194601000-00002

Francis P.T., Palmer A.M., Snape M., Wilcock G.K (1999) **The cholinergic hypothesis of Alzheimer's disease: a review of progress** *J. Neurol. Neurosurg. Psychiatry* **66**:137–147 https://doi.org/10.1136/jnnp.66.2.137

Froemke R.C., Merzenich M.M., Schreiner C.E (2007) **A synaptic memory trace for cortical receptive field plasticity** *Nature* **450**:425–429 https://doi.org/10.1038/nature06289

Fu Y., Tucciarone J.M., Espinosa J.S., Sheng N., Darcy D.P., Nicoll R.A., Huang Z.J., Stryker M.P (2014) **A Cortical Circuit for Gain Control by Behavioral State** *Cell* **156**:1139–1152 https://doi.org/10.1016/j.cell.2014.01.050

Gasselin C., Hohl B., Vernet A., Crochet S., Petersen C.C.H (2021) **Cell-type-specific nicotinic input disinhibits mouse barrel cortex during active sensing** *Neuron* **109**:778–787 https://doi.org/10.1016/j.neuron.2020.12.018

Goard M., Dan Y (2009) **Basal forebrain activation enhances cortical coding of natural scenes** *Nat. Neurosci* **12**:1444–1449 https://doi.org/10.1038/nn.2402

Granger A.J. *et al.* (2020) **Cortical ChAT+ neurons co-transmit acetylcholine and GABA in a target- and brain-region-specific manner** *eLife* **9** https://doi.org/10.7554/eLife.57749

Greuel J.M., Luhmann H.J., Singer W (1988) **Pharmacological Induction of Use-Dependent Receptive Field Modifications in the Visual Cortex** *Science* **242**:74–77 https://doi.org/10.1126/science.2902687

Gu Q., Singer W (1993) **Effects of intracortical infusion of anticholinergic drugs on neuronal plasticity in kitten striate cortex** *Eur. J. Neurosci* **5**:475–485 https://doi.org/10.1111/j.1460-9568.1993.tb00514.x

Gulledge A.T., Stuart G.J (2005) **Cholinergic Inhibition of Neocortical Pyramidal Neurons** *J. Neurosci* **25**:10308–10320 https://doi.org/10.1523/JNEUROSCI.2697-05.2005

Guo W., Robert B., Polley D.B (2019) **The Cholinergic Basal Forebrain Links Auditory Stimuli with Delayed Reinforcement to Support Learning** *Neuron* **103**:1164–1177 https://doi.org/10.1016/j.neuron.2019.06.024

Hampel H., Mesulam M.-M., Cuello A.C., Khachaturian A.S., Vergallo A., Farlow M.R., Snyder P.J., Giacobini E., Khachaturian Z.S (2019) **Revisiting the Cholinergic Hypothesis in Alzheimer's Disease: Emerging Evidence from Translational and Clinical Research** *J. Prev. Alzheimers Dis* **6**:2–15 https://doi.org/10.14283/jpad.2018.43

Hangya B., Ranade S.P., Lorenc M., Kepecs A (2015) **Central Cholinergic Neurons Are Rapidly Recruited by Reinforcement Feedback** *Cell* **162**:1155–1168 https://doi.org/10.1016/j.cell.2015.07.057

Harrison T.C., Pinto L., Brock J.R., Dan Y (2016) **Calcium Imaging of Basal Forebrain Activity during Innate and Learned Behaviors** *Front. Neural Circuits* **10** https://doi.org/10.3389/fncir.2016.00036

Hay Y.A., Lambolez B., Tricoire L (2016) **Nicotinic Transmission onto Layer 6 Cortical Neurons Relies on Synaptic Activation of Non-α7 Receptors** *Cereb. Cortex N. Y. N* **1991**:2549–2562 https://doi.org/10.1093/cercor/bhv085

Hedrick T., Waters J (2015) **Acetylcholine excites neocortical pyramidal neurons via nicotinic receptors** *J. Neurophysiol* **113**:2195–2209 https://doi.org/10.1152/jn.00716.2014

Heindorf M., Keller G.B (2022) **Reduction of layer 5 mediated long-range cortical communication by antipsychotic drugs** *bioRxiv* https://doi.org/10.1101/2022.01.31.478462

Held R., Hein A (1963) **Movement-produced stimulation in the development of visually guided behavior** *J. Comp. Physiol. Psychol* **56**:872–6

Jing M. *et al.* (2020) **An optimized acetylcholine sensor for monitoring in vivo cholinergic activity** *Nat. Methods* **17**:1139–1146 https://doi.org/10.1038/s41592-020-0953-2

Jordan R., Keller G.B (2023) **The locus coeruleus broadcasts prediction errors across the cortex to promote sensorimotor plasticity (preprint). elife** https://doi.org/10.7554/eLife.85111.1

Jordan R., Keller G.B (2020) **Opposing Influence of Top-down and Bottom-up Input on Excitatory Layer 2/3 Neurons in Mouse Primary Visual Cortex** *Neuron* **108**:1194–1206 https://doi.org/10.1016/j.neuron.2020.09.024

Kanamaru T., Aihara K (2019) **Acetylcholine-mediated top-down attention improves the response to bottom-up inputs by deformation of the attractor landscape** *PloS One* **14** https://doi.org/10.1371/journal.pone.0223592

Kaneko M., Stryker M.P (2014) **Sensory experience during locomotion promotes recovery of function in adult visual cortex** *eLife* **3** https://doi.org/10.7554/eLife.02798

Keller G.B., Bonhoeffer T., Hübener M (2012) **Sensorimotor mismatch signals in primary visual cortex of the behaving mouse** *Neuron* **74**:809–15 https://doi.org/10.1016/j.neuron.2012.03.040

Keller G.B., Mrsic-Flogel T.D (2018) **Predictive Processing: A Canonical Cortical Computation** *Neuron* **100**:424–435 https://doi.org/10.1016/j.neuron.2018.10.003

Kilgard M.P., Merzenich M.M (1998) **Cortical map reorganization enabled by nucleus basalis activity** *Science* **279**:1714–1718 https://doi.org/10.1126/science.279.5357.1714

Kim J.-H., Jung A.-H., Jeong D., Choi I., Kim K., Shin S., Kim S.J., Lee S.-H (2016) **Selectivity of Neuromodulatory Projections from the Basal Forebrain and Locus Ceruleus to Primary Sensory Cortices** *J. Neurosci* **36**:5314–5327 https://doi.org/10.1523/JNEUROSCI.4333-15.2016

Kirkwood A., Rozas C., Kirkwood J., Perez F., Bear M.F (1999) **Modulation of long-term synaptic depression in visual cortex by acetylcholine and norepinephrine** *J. Neurosci* **19**:1599–1609 https://doi.org/10.1523/jneurosci.19-05-01599.1999

Klapoetke N.C. *et al.* (2014) **Independent optical excitation of distinct neural populations** *Nat. Methods* **11**:338–346 https://doi.org/10.1038/nmeth.2836

Korzhova V., Marinković P., Njavro J.R., Goltstein P.M., Sun F., Tahirovic S., Herms J., Liebscher S (2021) **Long-term dynamics of aberrant neuronal activity in awake Alzheimer's disease transgenic mice. Commun** *Biol* **4** https://doi.org/10.1038/s42003-021-02884-7

Krnjević K., Phillis J.W (1963) **Acetylcholine-sensitive cells in the cerebral cortex** *J. Physiol* **166**:296–327 https://doi.org/10.1113/jphysiol.1963.sp007106

Larsen R.S., Turschak E., Daigle T., Zeng H., Zhuang J., Waters J (2018) **Activation of neuromodulatory axon projections in primary visual cortex during periods of locomotion and pupil dilation** *bioRxiv* :502013–502013 https://doi.org/10.1101/502013

Laszlovszky T., Schlingloff D., Hegedüs P., Freund T.F., Gulyás A., Kepecs A., Hangya B (2020) **Distinct synchronization, cortical coupling and behavioral function of two basal forebrain cholinergic neuron types** *Nat. Neurosci* https://doi.org/10.1038/s41593-020-0648-0

Lee A.M., Hoy J.L., Bonci A., Wilbrecht L., Stryker M.P., Niell C.M (2014) **Identification of a Brainstem Circuit Regulating Visual Cortical State in Parallel with Locomotion** *Neuron* **83**:455–466 https://doi.org/10.1016/J.NEURON.2014.06.031

Leinweber M., Ward D.R., Sobczak J.M., Attinger A., Keller G.B (2017) **A Sensorimotor Circuit in Mouse Cortex for Visual Flow Predictions** *Neuron* **95**:1420–1432 https://doi.org/10.1016/j.neuron.2017.08.036

Leinweber M., Zmarz P., Buchmann P., Argast P., Hübener M., Bonhoeffer T., Keller G.B (2014) **Two-photon calcium imaging in mice navigating a virtual reality environment** *J. Vis. Exp. JoVE e* **50885** https://doi.org/10.3791/50885

Li X. *et al.* (2018) **Generation of a whole-brain atlas for the cholinergic system and mesoscopic projectome analysis of basal forebrain cholinergic neurons** *Proc. Natl. Acad. Sci. U. S. A* **115**:415–420 https://doi.org/10.1073/pnas.1703601115

Lohani S., Moberly A.H., Benisty H., Landa B., Jing M., Li Y., Higley M.J., Cardin J.A (2022) **Spatiotemporally heterogeneous coordination of cholinergic and neocortical activity** *Nat. Neurosci* **25**:1706–1713 https://doi.org/10.1038/s41593-022-01202-6

Metherate R., Weinberger N.M (1990) **Cholinergic modulation of responses to single tones produces tone-specific receptive field alterations in cat auditory cortex** *Synapse* **6**:133–145 https://doi.org/10.1002/syn.890060204

Minces V., Pinto L., Dan Y., Chiba A.A (2017) **Cholinergic shaping of neural correlations** *Proc. Natl. Acad. Sci. U. S. A* **114**:5725–5730 https://doi.org/10.1073/pnas.1621493114

Nelson A., Mooney R (2016) **The Basal Forebrain and Motor Cortex Provide Convergent yet Distinct Movement-Related Inputs to the Auditory Cortex** *Neuron* **90**:635–648 https://doi.org/10.1016/j.neuron.2016.03.031

Niell C.M., Stryker M.P (2010) **Modulation of Visual Responses by Behavioral State in Mouse Visual Cortex** *Neuron* **65**:472–479 https://doi.org/10.1016/j.neuron.2010.01.033

Niell C.M., Stryker M.P (2008) **Highly Selective Receptive Fields in Mouse Visual Cortex** *J. Neurosci* **28**:7520–7536 https://doi.org/10.1523/JNEUROSCI.0623-08.2008

Obermayer J., Verhoog M.B., Luchicchi A., Mansvelder H.D (2017) **Cholinergic modulation of cortical microcircuits is layer-specific: Evidence from rodent, monkey and human brain** *Front. Neural Circuits* **11** https://doi.org/10.3389/fncir.2017.00100

Pafundo D.E., Nicholas M.A., Zhang R., Kuhlman S.J (2016) **Top-Down-Mediated Facilitation in the Visual Cortex Is Gated by Subcortical Neuromodulation** *J. Neurosci* **36**:2904–2914 https://doi.org/10.1523/JNEUROSCI.2909-15.2016

Pakan J.M., Lowe S.C., Dylda E., Keemink S.W., Currie S.P., Coutts C.A., Rochefort N.L (2016) **Behavioral-state modulation of inhibition is context-dependent and cell type specific in mouse visual cortex** *eLife* **5** https://doi.org/10.7554/eLife.14985

Perry E.K., Tomlinson B.E., Blessed G., Bergmann K., Gibson P.H., Perry R.H (1978) **Correlation of cholinergic abnormalities with senile plaques and mental test scores in senile dementia** *Br. Med. J* **2**:1457–1459

Pinto L., Goard M.J., Estandian D., Xu M., Kwan A.C., Lee S.-H., Harrison T.C., Feng G., Dan Y (2013) **Fast modulation of visual perception by basal forebrain cholinergic neurons** *Nat. Neurosci. 2013* **1612**:1857–1857 https://doi.org/10.1038/nn.3552

Polack P.-O., Friedman J., Golshani P (2013) **Cellular mechanisms of brain state–dependent gain modulation in visual cortex** *Nat. Neurosci* **16**:1331–1339 https://doi.org/10.1038/nn.3464

Rasmusson D.D., Dykes R.W (1988) **Long-term enhancement of evoked potentials in cat somatosensory cortex produced by co-activation of the basal forebrain and cutaneous receptors** *Exp. Brain Res* **70**:276–286 https://doi.org/10.1007/BF00248353

Reimer J., Froudarakis E., Cadwell C.R., Yatsenko D., Denfield G.H., Tolias A.S (2014) **Pupil Fluctuations Track Fast Switching of Cortical States during Quiet Wakefulness** *Neuron* **84**:355–362 https://doi.org/10.1016/j.neuron.2014.09.033

Reimer J., McGinley M.J., Liu Y., Rodenkirch C., Wang Q., McCormick D.A., Tolias A.S (2016) **Pupil fluctuations track rapid changes in adrenergic and cholinergic activity in cortex** *Nat. Commun* https://doi.org/10.1038/ncomms13289

Ren C., Peng K., Yang R., Liu W., Liu C., Komiyama T (2022) **Global and subtype-specific modulation of cortical inhibitory neurons regulated by acetylcholine during motor learning** *Neuron* **110**:2334–2350 https://doi.org/10.1016/j.neuron.2022.04.031

Robert B., Kimchi E.Y., Watanabe Y., Chakoma T., Jing M., Li Y., Polley D.B (2021) **A functional topography within the cholinergic basal forebrain for encoding sensory cues and behavioral reinforcement outcomes** *eLife* **10** https://doi.org/10.7554/eLife.69514

Rossi J., Balthasar N., Olson D., Scott M., Berglund E., Lee C.E., Choi M.J., Lauzon D., Lowell B.B., Elmquist J.K (2011) **Melanocortin-4-receptors Expressed by Cholinergic Neurons Regulate Energy Balance and Glucose Homeostasis** *Cell Metab* **13**:195–204 https://doi.org/10.1016/j.cmet.2011.01.010

Sachdev R.N.S., Lu S.-M., Wiley R.G., Ebner F.F (1998) **Role of the Basal Forebrain Cholinergic Projection in Somatosensory Cortical Plasticity** *J. Neurophysiol* **79**:3216–3228 https://doi.org/10.1152/jn.1998.79.6.3216

Saleem A.B., Ayaz A., Jeffery K.J., Harris K.D., Carandini M (2013) **Integration of visual motion and locomotion in mouse visual cortex** *Nat. Neurosci* **16**:1864–9 https://doi.org/10.1038/nn.3567

Saravanan V., Berman G.J., Sober S.J. (2020) **Application of the hierarchical bootstrap to multi-level data in neuroscience**

Sato H., Hata Y., Masui H., Tsumoto T (1987) **A functional role of cholinergic innervation to neurons in the cat visual cortex** *J. Neurophysiol* **58**:765–780 https://doi.org/10.1152/jn.1987.58.4.765

Sillito A.M., Kemp J.A (1983) **Cholinergic modulation of the functional organization of the cat visual cortex** *Brain Res* **289**:143–155 https://doi.org/10.1016/0006-8993(83)90015-X

Soma S., Shimegi S., Suematsu N., Tamura H., Sato H (2013) **Modulation-specific and laminar-dependent effects of acetylcholine on visual responses in the rat primary visual cortex** *PloS One* **8** https://doi.org/10.1371/journal.pone.0068430

Suzuki M., Larkum M.E (2020) **General Anesthesia Decouples Cortical Pyramidal Neurons** *Cell* **180**:666–676 https://doi.org/10.1016/j.cell.2020.01.024

Terry A.V., Buccafusco J.J (2003) **The cholinergic hypothesis of age and Alzheimer's disease-related cognitive deficits: recent challenges and their implications for novel drug development** *J. Pharmacol. Exp. Ther* **306**:821–827 https://doi.org/10.1124/jpet.102.041616

Tsuchiya R., Yoshiki F., Kudo Y., Morita M (2002) **Cell type-selective expression of green fluorescent protein and the calcium indicating protein, yellow cameleon, in rat cortical primary cultures** *Brain Res* **956**:221–229 https://doi.org/10.1016/S0006-8993(02)03518-7

Unal C.T., Golowasch J.P., Zaborszky L (2012) **Adult mouse basal forebrain harbors two distinct cholinergic populations defined by their electrophysiology** *Front. Behav. Neurosci* **6**:21–21 https://doi.org/10.3389/fnbeh.2012.00021

Vasilevskaya A., Widmer F.C., Keller G.B., Jordan R (2023) **Locomotion-induced gain of visual responses cannot explain visuomotor mismatch responses in layer 2/3 of primary visual cortex** *Cell Rep* **42** https://doi.org/10.1016/j.celrep.2023.112096

Vinck M., Batista-Brito R., Knoblich U., Cardin J.A (2015) **Arousal and Locomotion Make Distinct Contributions to Cortical Activity Patterns and Visual Encoding** *Neuron* **86**:740–754 https://doi.org/10.1016/j.neuron.2015.03.028

Widmer F.C., O'Toole S.M., Keller G.B (2022) **NMDA receptors in visual cortex are necessary for normal visuomotor integration and skill learning** *eLife* **11** https://doi.org/10.7554/eLife.71476

Wilson D.A., Fletcher M.L., Sullivan R.M (2004) **Acetylcholine and Olfactory Perceptual Learning** *Learn. Mem* **11**:28–34 https://doi.org/10.1101/lm.66404

Xiang Z (1998) **Cholinergic Switching Within Neocortical Inhibitory Networks** *Science* **281**:985–988 https://doi.org/10.1126/science.281.5379.985

Yaguchi M., Ohashi Y., Tsubota T., Sato A., Koyano K.W., Wang N., Miyashita Y (2013) **Characterization of the Properties of Seven Promoters in the Motor Cortex of Rats and Monkeys After Lentiviral Vector-Mediated Gene Transfer** *Hum. Gene Ther. Methods* **24**:333–344 https://doi.org/10.1089/hgtb.2012.238

Zhu F., Elnozahy S., Lawlor J., Kuchibhotla K.V (2023) **The cholinergic basal forebrain provides a parallel channel for state-dependent sensory signaling to auditory cortex** *Nat. Neurosci* :1–10 https://doi.org/10.1038/s41593-023-01289-5

Zolles G., Wagner E., Lampert A., Sutor B (2009) **Functional expression of nicotinic acetylcholine receptors in rat neocortical layer 5 pyramidal cells** *Cereb. Cortex N. Y. N* **1991**:1079–1091 https://doi.org/10.1093/cercor/bhn158

Article and author information

Baba Yogesh
Friedrich Miescher Institute for Biomedical Research, Basel, Switzerland, Faculty of Natural Sciences, University of Basel, Basel, Switzerland

Georg B. Keller
Friedrich Miescher Institute for Biomedical Research, Basel, Switzerland, Faculty of Natural Sciences, University of Basel, Basel, Switzerland
For correspondence: georg.keller@fmi.ch
ORCID iD: 0000-0002-1401-0117

Copyright

Editors

Reviewing Editor
Naoshige Uchida
Harvard University, Cambridge, United States of America

Senior Editor
Tirin Moore
Howard Hughes Medical Institute, Stanford University, Stanford, United States of America

Reviewer #1 (Public Review):

The paper submitted by Yogesh and Keller explores the role of cholinergic input from the basal forebrain (BF) in the mouse primary visual cortex (V1). The study aims to understand the signals conveyed by BF cholinergic axons in the visual cortex, their impact on neurons in different cortical layers, and their computational significance in cortical visual processing. The authors employed two-photon calcium imaging to directly monitor cholinergic input from BF axons expressing GCaMP6 in mice running through a virtual corridor, revealing a strong correlation between BF axonal activity and locomotion. This persistent activation during locomotion suggests that BF input provides a binary locomotion state signal. To elucidate the impact of cholinergic input on cortical activity, the authors conducted optogenetic and chemogenetic manipulations, with a specific focus on L2/3 and L5 neurons. They found that cholinergic input modulates the responses of L5 neurons to visual stimuli and visuomotor mismatch, while not significantly affecting L2/3 neurons. Moreover, the study demonstrates that BF cholinergic input leads to decorrelation in the activity patterns of L2/3 and L5 neurons.

This topic has garnered significant attention in the field, drawing the interest of many researchers actively investigating the role of BF cholinergic input in cortical activity and sensory processing. The experiments and analyses were thoughtfully designed and conducted with rigorous standards, leading to convincing results which align well with findings in previous studies. In other words, some of the main findings, such as the correlation between cholinergic input and locomotor activity and the effects of cholinergic input on V1 cortical activity, have been previously demonstrated by other labs (Goard and Dan, 2009; Pinto et al., 2013; Reimer et al., 2016). However, the study by Yogesh and Keller stands out by combining cutting-edge calcium imaging and optogenetics to provide compelling evidence of layer-specific differences in the impact of cholinergic input on neuronal responses to bottom-up (visual stimuli) and top-down inputs (visuomotor mismatch).

https://doi.org/10.7554/eLife.89986.2.sa1

Reviewer #2 (Public Review):

The manuscript investigates the function of basal forebrain cholinergic axons in mouse primary visual cortex (V1) during locomotion using two-photon calcium imaging in head-fixed mice. Cholinergic modulation has previously been proposed to mediate the effects of locomotion on V1 responses. The manuscript concludes that the activity of basal forebrain cholinergic axons in visual cortex provides a signal which is more correlated with binary locomotion state than locomotion velocity of the animal. Cholinergic axons did not seem to respond to grating stimuli or visuomotor prediction error. Optogenetic stimulation of these axons increased the amplitude of responses to visual stimuli and decreased the response latency of layer 5 excitatory neurons, but not layer 2/3 neurons. Moreover, optogenetic or chemogenetic stimulation of cholinergic inputs reduced pairwise correlation of neuronal responses. These results provide insight into the role of cholinergic modulation to visual cortex and demonstrate that it affects different layers of visual cortex in a distinct manner. The experiments are well executed and the data appear to be of high quality. However, further analyses are required to fully support some of the study's conclusions.

The manuscript concludes that cholinergic axons convey a binary locomotion signal and are not tuned to running speed. Getting head-fixed animals to run at the speeds typical of freely moving animals can require training, which was not undertaken in this study. Consequently, the typically low running velocity of mice is a potential limitation of this study.

The analyses of the effects of locomotion and stimulation of cholinergic inputs present grand averages of responses across all neurons, and therefore may mask heterogeneity across layer 2/3 and layer 5 neurons.

https://doi.org/10.7554/eLife.89986.2.sa0

Author Response

We thank you for the time you took to review our work and for your feedback!

The major changes to the manuscript are:

1. We have extended the range of locomotion velocity over which we compare its dependence with cholinergic activity in Figures 2E and S2H.
2. We have quantified the contributions of cholinergic stimulation on multiplicative and additive gains on visual responses (Figure S7).
3. We have provided single cell examples for the change in latency to visual response (Figure S12).
4. We have added an analysis to compare layer 2/3 and layer 5 locomotion onset responses as a function of visuomotor condition (Figure S8).

A detailed point-by-point response to all reviewer concerns is provided below.

> ***Reviewer #1 (Public Review):***
>
> *The paper submitted by Yogesh and Keller explores the role of cholinergic input from the basal forebrain (BF) in the mouse primary visual cortex (V1). The study aims to understand the signals conveyed by BF cholinergic axons in the visual cortex, their impact on neurons in different cortical layers, and their computational significance in cortical visual processing. The authors employed two-photon calcium imaging to directly monitor cholinergic input from BF axons expressing GCaMP6 in mice running through a virtual corridor, revealing a strong correlation between BF axonal activity and locomotion. This persistent activation during locomotion suggests that BF input provides a binary locomotion state signal. To elucidate the impact of cholinergic input on cortical activity, the authors conducted optogenetic and chemogenetic manipulations, with a specific focus on L2/3 and L5 neurons. They found that cholinergic input modulates the responses of L5 neurons to visual stimuli and visuomotor mismatch, while not significantly affecting L2/3 neurons. Moreover, the study demonstrates that BF cholinergic input leads to decorrelation in the activity patterns of L2/3 and L5 neurons.*
>
> *This topic has garnered significant attention in the field, drawing the interest of many researchers actively investigating the role of BF cholinergic input in cortical activity and sensory processing. The experiments and analyses were thoughtfully designed and conducted with rigorous standards, leading to convincing results which align well with findings in previous studies. In other words, some of the main findings, such as the correlation between cholinergic input and locomotor activity and the effects of cholinergic input on V1 cortical activity, have been previously demonstrated by other labs (Goard and Dan, 2009; Pinto et al., 2013; Reimer et al., 2016). However, the study by Yogesh and Keller stands out by combining cutting-edge calcium imaging and optogenetics to provide compelling evidence of layerspecific differences in the impact of cholinergic input on neuronal responses to bottom-up (visual stimuli) and top-down inputs (visuomotor mismatch).*

We thank the reviewer for their feedback.

> ***Reviewer #2 (Public Review):***
>
> *The manuscript investigates the function of basal forebrain cholinergic axons in mouse primary visual cortex (V1) during locomotion using two-photon calcium imaging in head-fixed mice. Cholinergic modulation has previously been proposed to mediate the effects of locomotion on V1 responses. The manuscript concludes that the activity of basal forebrain cholinergic axons in visual cortex provides a signal which is more correlated with binary locomotion state than locomotion velocity of the animal. Cholinergic axons did not seem to respond to grating stimuli or visuomotor prediction error. Optogenetic stimulation of these axons increased the amplitude of responses to visual stimuli and decreased the response latency of layer 5 excitatory neurons, but not layer 2/3 neurons. Moreover, optogenetic or chemogenetic stimulation of cholinergic inputs reduced pairwise correlation of neuronal responses. These results provide insight into the role of cholinergic modulation to visual cortex and demonstrate that it affects different layers of visual cortex in a distinct manner. The experiments are well executed and the data appear to be of high quality. However, further analyses are required to fully support several of the study's conclusions.*

We thank the reviewer for their feedback.

> 1. *In experiments analysing the activity of V1 neurons, GCaMP6f was expressed using a ubiquitous Ef1a promoter, which is active in all neuronal cell types as well as potentially non-neuronal cells. The manuscript specifically refers to responses of excitatory neurons but it is unclear how excitatory neuron somata were identified and distinguished from that of inhibitory neurons or other cell types.*

This might be a misunderstanding. The Ef1α promoter has been reported to drive highly specific expression in neurons (Tsuchiya et al., 2002) with 99.7% of labeled cells in layer 2/3 of rat cortex being NeuN+ (a neuronal marker), with only 0.3% of labeled cells being GFAP+ (a glial marker) (Yaguchi et al., 2013). This bias was even stronger in layer 5 with 100% of labeled cells being NeuN+ and none GFAP+ (Yaguchi et al., 2013). The Ef1α promoter in an AAV vector, as we use it here, also biases expression to excitatory neurons. In layer 2/3 of mouse visual cortex, we have found that 96.8% ± 0.7% of labeled neurons are excitatory three weeks after viral injection (Attinger et al., 2017). Similar results have also been found in rats (Yaguchi et al., 2013), where on expressing GFP under Ef1a promoter delivered using Lenti virus, 95.2% of labeled neurons in layer 2/3 were excitatory and 94.1% in layer 5 were excitatory. These numbers are comparable to the ones obtained with promoters commonly used to target expression to excitatory neurons. To do this, typically two variants of promoters based on the transcription start region of CaMKIIα gene have been used. The first, the CaMKIIα-0.4 promoter, results in 95% excitatory specificity (Scheyltjens et al., 2015). The second, the CaMKIIα-1.3 promoter, results in only 82% excitatory specificity (Scheyltjens et al., 2015), and is thus not far from chance. We have clarified this in the manuscript. Nevertheless, we have removed the qualifier “excitatory” when talking about neurons in most instances, throughout the manuscript.

> 1. *The manuscript concludes that cholinergic axons convey a binary locomotion signal and are not tuned to running speed. The average running velocity of mice in this study is very slow - slower than 15 cm/s in the example trace in Figure 1D and speeds <6 cm/s were quantified in Figure 2E. However, mice can run at much faster speeds both under head-fixed and freely moving conditions (see e.g. Jordan and Keller, 2020, where example running speeds are ~35 cm/s). Given that the data in the present manuscript cover such a narrow range of running speeds, it is not possible to determine whether cholinergic axons are tuned to running speed or convey a binary locomotion signal.*

Our previous analysis window of 0-6.25 cm/s covered approximately 80% of all data. We have increased the analysis window to 0-35 cm/s that now covers more than 99% of the data (see below). Also, note that very high running speeds are probably overrepresented in the Jordan and Keller 2020 paper as mice had to be trained to run reliably before all experiments given the relatively short holding times of the intracellular recordings. The running speeds in our current dataset are comparable to other datasets we have acquired in similar experiments.

Figure 2E has now been updated to reflect the larger range of data. Please note, as the number of mice that contribute to the data now differs as a function of velocity (some mice run faster than others), we have now switched to a variant of the plot based on hierarchical bootstrap sampling (see Methods). This does not overtly change the appearance of the plot. See Author response image 1 for a comparison of the original plot, the extended range without bootstrap sampling, and the extended range with bootstrap sampling currently used in the paper.

Author response image 1.

Average activity of cholinergic axons as a function of locomotion velocity. (A) As in the previous version of the manuscript. (B) As in A, but with the extended velocity range. (C) As in B, but using hierarchical bootstrap sampling to estimate median (red dots) and 95% confidence interval (shading) for each velocity bin.

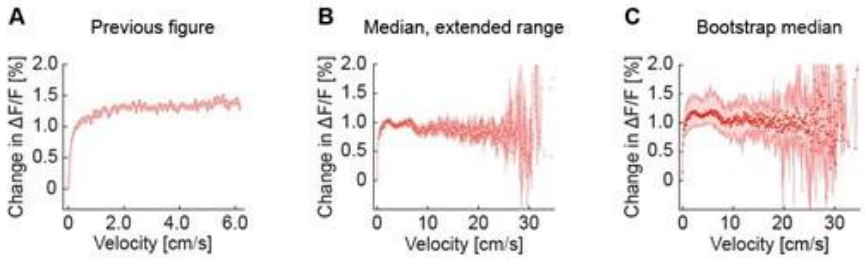

> 1. *The analyses in Figure 4 only consider the average response to all grating orientations and directions. Without further analysing responses to individual grating directions it is unclear how stimulation of cholinergic inputs affects visual responses. Previous work (e.g. Datarlat and Stryker, 2017) has shown that locomotion can have both additive and multiplicative effects and it would be valuable to determine the type of modulation provided by cholinergic stimulation.*

We thank the reviewer for this suggestion. To address this, we quantified how cholinergic stimulation influenced the orientation tuning of V1 neurons. The stimuli we used were full field sinusoidal drifting gratings of 4 different orientations (2 directions each). For each neuron, we identified the preferred orientation and plotted responses relative to this

preferred orientation as a function of whether the mouse was running, or we were stimulating cholinergic axons. Consistent with previous work, we found a mixture of a multiplicative and an additive components during running. With cholinergic axon stimulation, the multiplicative effect was stronger than the additive effect. This is now quantified in Figure S7.

> 1. *The difference between the effects of locomotion and optogenetic stimulation of cholinergic axons in Figure 5 may be confounded by differences in the visual stimulus. These experiments are carried out under open-loop conditions, where mice may adapt their locomotion based on the speed of the visual stimulus. Consequently, locomotion onsets are likely to occur during periods of higher visual flow. Since optogenetic stimulation is presented randomly, it is likely to occur during periods of lower visual flow speed. Consequently, the difference between the effect of locomotion and optogenetic stimulation may be explained by differences in visual flow speed and it is important to exclude this possibility.*

We find that in general locomotion is unaffected by visual flow in open loop conditions in this type of experiment (in this particular dataset, there was a small negative correlation between locomotion and visual flow in the open loop condition, Author response image 2).

Author response image 2.

Correlation between visual flow and locomotion in open loop conditions. Average correlation of locomotion velocity and visual flow speed in open loop for all mice in Figure 5. Each dot is an imaging site. In the open loop, the correlation between locomotion and visual flow speed is close to zero, but significantly negative in this dataset.

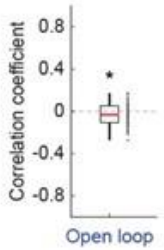

However, to directly address the concern that our results are influenced by visual flow, we can restrict our analysis only to locomotion onsets that occurred in absence of visual flow (Author response image 3A and R3B). These responses are not substantially different from those when including all data (Figures 5A and 5B). Thus, the difference between the effect of locomotion and optogenetic stimulation cannot be explained by differences in visual flow speed.

Author response image 3.

Open loop locomotion onset responses without visual flow. (A) Average calcium response of layer 2/3 neurons in visual cortex to locomotion onset in open loop in the absence of visual flow. Shading indicates SEM. (B) As in A, but for layer 5 neurons.

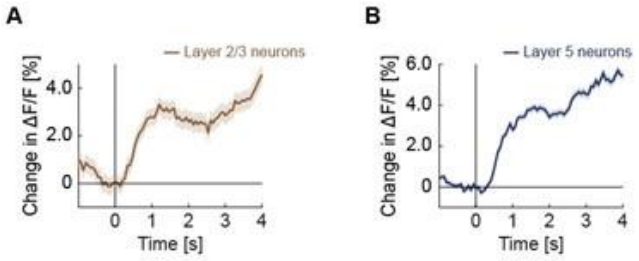

> *1. It is unclear why chemogenetic manipulations of cholinergic inputs had no effect on pairwise correlations of L2/3 neuronal responses while optogenetic stimulation did.*

This is correct – we do not know why that is the case and can only speculate. There are at least two possible explanations for this difference:

1. Local vs. systemic. The optogenetic manipulation is relatively local, while the chemogenetic manipulation is systemic. It is not clear how cholinergic release in other brain regions influences the correlation structure in visual cortex. It is conceivable that a cortex-wide change in cholinergic release results in a categorically different state with a specific correlation structure in layer 2/3 neurons different from the one induced by the more local optogenetic manipulation.

2. Layer-specificity of activation. Cholinergic projections to visual cortex arrive both in superficial and deep layers. We activate the axons in visual cortex optogenetically by illuminating the cortical surface. Thus, in our optogenetic experiments, we are primarily activating the axons arriving superficially, while in the chemogenetic experiment, we are likely influencing superficial and deep axons similarly. Thus, we might expect a bias in the optogenetic activation to influencing superficial layers more strongly than the chemogenetic activation does.

> *1. The effects of locomotion and optogenetic stimulation on the latency of L5 responses in Figure 7 are very large - ~100 ms. Indeed, typical latencies in mouse V1 measured using electrophysiology are themselves shorter than 100 ms (see e.g. Durand et al., 2016). Visual response latencies in stationary conditions or without optogenetic stimulation appear surprisingly long - much longer than reported in previous studies even under anaesthesia. Such large and surprising results require careful analysis to ensure they are not confounded by artefacts. However, as in Figure 4, this analysis is based only on average responses across all gratings and no individual examples are shown.*

This is correct and we speculate this is the consequence of a combination of different reasons.

1. Calcium imaging is inherently slower than electrophysiological recordings. While measuring spiking responses using electrophysiology, response latencies of on the order of 100 ms have indeed been reported, as the reviewer points out. Using calcium imaging these latencies are typically 4 times longer (Kuznetsova et al., 2021). This is likely a combination of a) calcium signals that are slower than electrical changes, b) delays in the calcium sensor itself, and c) temporal sampling used for imaging that is about 3 orders of magnitude slower than what typically used for electrophysiology.

2. Different neurons included in analysis. The calcium imaging likely has very different biases than electrophysiological recordings. Historically, the fraction of visually responsive neurons in visual cortex based on extracellular electrophysiological recordings has been systematically overestimated (Olshausen and Field, 2005). One key contributor to this is the fact that recordings are biased to visually responsive neurons. The criteria for inclusion of “responsive neurons” strongly influences the “average” response latency. In addition, calcium imaging has biases that relate to the vertical position of the somata in cortex. Both layer 2/3 and layer 5 recordings are likely biased to superficial layer 2/3 and superficial layer 5 neurons. Conversely, electrical recordings are likely biased to layer 4 and layer 5 neurons. Thus, comparisons at this level of resolution between data obtained with these two methods are difficult to make.

We have added example neurons as Figure S12, as suggested.

> ***Reviewer #1 (Recommendations For The Authors):***
>
> *While the study showcases valuable insights, I have a couple of concerns regarding the novelty of their research and the interpretation of results. By addressing these concerns, the authors can clarify the positioning of their research and strengthen the significance of their findings.*
>
> *(Major comments)*
>
> 1. *Page 1, Line 21: The authors claim, "Our results suggest that acetylcholine augments the responsiveness of layer 5 neurons to inputs from outside of the local network, enabling faster switching between internal representations during locomotion." However, it is not clear which specific data or results support the claim of "switching between internal representations." Overall, their study primarily presents responses averaged across all neurons imaged, lacking a detailed exploration of individual neuron response patterns. Population analysis, such as PCA and decoding, can be used to assess the encoding of each stimulus by V1 neurons - "internal representation."*
> *To strengthen their claim regarding "switching between internal representations," the authors could consider an experiment measuring the speed at which the population activity pattern A transitions to the population activity pattern B when the visual stimulus switches from A to B. Such experiments would significantly enhance the impact of their study, providing a clearer understanding of how BF cholinergic input influences the dynamic representation of stimuli during locomotion.*

We thank the reviewer for bringing this up. That acetylcholine enables a faster switching between internal representations in layer 5 is a speculation. We have attempted to make this clearer in the discussion. Our speculation is based on the finding that the population response in layer 5 to sensory input is faster under high levels of acetylcholine (Figures 4D and 7B). In line with the reviewer’s intuition, the neuronal response to a change in visual stimulus, in our experiment from a uniform grey visual stimulus to a sinusoidal grating stimulus, is indeed faster. Based on evidence in favor of layer 5 encoding internal representation (Heindorf and Keller, 2023; Keller and Mrsic-Flogel, 2018; Suzuki and Larkum, 2020), we interpret the decrease in latency of the population response as a faster change in internal representation. We are not sure a decoding analysis would add much to this, given that a trivial decoder simply based on mean population response would already find a faster transition. We have expanded on our explanation of these points in the manuscript.

> 1. *Page 4, Line 103: "..., a direct measurement of the activity of cholinergic projection from basal forebrain to the visual cortex during locomotion has not been made." This statement is incorrect. An earlier study by Reimer et al. indeed imaged cholinergic axons in the visual cortex of mice running on a wheel. They found that "After walking onset, ... ACh activation, and a large pupil diameter, were sustained throughout the walking period in both cortical areas V1 and A1." Their findings are very similar to the results presented by Yogesh and Keller - that is, BF cholinergic axons exhibited locomotion statedependent activity. The authors should clarify the positioning of this study relative to previous studies.*
>
> *Reimer, J., McGinley, M., Liu, Y. et al. Pupil fluctuations track rapid changes in adrenergic and cholinergic activity in cortex. Nat Commun 7, 13289 (2016). https://doi.org/10.1038/ncomms13289*

We have clarified this as suggested. However, we disagree slightly with the reviewer here. The key question is whether the cholinergic axons imaged originate in basal forebrain. While Reimer et al. 2016 did set out to do this, we believe a number of methodological considerations prevent this conclusion:

1. In their analysis, Reimer et al. 2016 combine data from mice with cholinergic axons labeled with either viral injection to basal forebrain or germline cross of ChAT-cre mice with reporter line. Unfortunately, it is unclear what the exact number of mice labeled with either strategy was. Based on the information in the paper, we can conclude that of the 6 mice used for experiments between 2 and 5 were germline cross. The problem with germline labeling of ChAT positive neurons is that when using a cross, VIP-ChAT+ neurons in cortex are also labeled. Based on the fact that Reimer et al. 2016 find an anticipatory increase in activity on locomotion onset, that is also seen by Larsen et al. 2018 (they use a germline cross strategy), an effect we do not see in our data, we speculate that a significant part of the signals reported in the Reimer et al. 2016 paper are from local VIP-ChAT+ neurons.

2. In their analysis, Reimer et al. 2016 also combine all imaging data obtained from both primary auditory cortex and primary visual cortex. Given the heterogeneity in the basal forebrain cholinergic neuronal population and their projection selectivity, to better understand these signals, it's important to acquire the signals from cholinergic axons selectively in specific cortical regions, which we do in visual cortex. Based on the information provided in their paper, we were unfortunately not able to discern the injection location for their viral labeling strategy. Given the topographic selectivity in projection from basal forebrain, this could give hints as to the relative contribution of cholinergic projections to A1 vs V1 in their data. The injection coordinates given in the methods of the Reimer paper, of 4 mm lateral and 0.5 mm posterior to bregma to target basal forebrain, are likely wrong (they fall outside the head of the mouse).

Given the heterogeneity in the basal forebrain cholinergic neuronal population and their projection selectivity, to better understand these signals, it's important to acquire the signals from cholinergic axons both selectively in a cortical region, as we do in visual cortex, and purely originating from basal forebrain. Collins et al. 2023 inject more laterally and thus characterize cholinergic input to S1 and A1, while Lohani et al. 2022 use GRAB sensors which complement our findings. Please note, we don't think there is any substantial disagreement in the results of previous studies and ours, with very few exceptions, like the anticipatory increase in cholinergic activity that precedes locomotion onset in the Reimer et al. 2016 data, but not in ours. This is a rather critical point in the context of the literature of motor-related neuronal activity in mouse V1. Based on early work on the topic, it is frequently assumed that

motor-related activity in V1 is driven by a cholinergic input. This is very likely incorrect given our results, hence we feel it is important to highlight this methodological caveat of earlier work.

> 1. *Fig. 4H: The authors found that L5 neurons exhibit positive responses at the onset of locomotion in a closed-loop configuration. Moreover, these responses are further enhanced by photostimulation of BF axons.*
>
> *In a previous study from the same authors' group (Heindorf and Keller, 2023), they reported 'negative' responses in L5a IT neurons during closed-loop locomotion. This raises a question about the potential influence of different L5 neuron types on the observed results between the two studies. Do the author think that the involvement of the other neuronal type in L5, the PT neurons, might explain the positive responses seen in the present study? Discussing this point in the paper would provide valuable insights into the underlying mechanisms.*

Yes, we do think the positive response observed on locomotion onset in closed loop is due to non-Tlx3+ neurons. Given that Tlx3-cre only labels a subset of inter-telencephalic (IT) neurons (Gerfen et al., 2013; Heindorf and Keller, 2023), it's not clear whether the positive response is explained by the pyramidal tract (PT) neurons, or the non-Tlx3+ IT neurons. Dissecting the response profiles of different subsets of layer 5 neurons is an active area of research in the lab and we hope to be able to answer these points more comprehensively in future publications. We have expanded on this in the discussion as suggested.

> *Furthermore, it would be valuable to investigate whether the effects of photostimulation of BF axons vary depending on neuronal responsiveness. This could help elucidate how neurons with positive responses, potentially putative PT neurons, differ from neurons with negative responses, putative IT neurons, in their response to BF axon photostimulation during locomotion.*

We have attempted an analysis of the form suggested. In short, we found no relationship between a neuron's response to optogenetic stimulation of ChAT axons and its response to locomotion onset, or its mean activity. Based on their response to locomotion onset in closed loop, we split layer 5 neurons into three groups, 30% most strongly decreasing (putative Tlx3+), 30% most strongly increasing, and the rest. We did not see a response to optogenetic stimulation of basal forebrain cholinergic axons in any of the three groups (Author response image 4A). We also found no obvious relationship between the mean activity of neurons and their response to optogenetic stimulation (Author response image 4B).

Author response image 4.

Neither putative layer 5 cell types nor neuronal responsiveness correlates with the response to optogenetic stimulation of cholinergic axons. (A) Average calcium response of layer 5 neurons split into putative Tlx3 (closed loop locomotion onset suppressed) and non-Tlx3 like (closed loop locomotion onset activated) to optogenetic stimulation of cholinergic axons. (B) Average calcium response of layer 5 neurons to optogenetic stimulation of cholinergic axons as a function of their mean response throughout the experimental session. Left: Each dot is a neuron. Right: Average correlation in the response of layer 5 to optogenetic stimulation and mean activity over all neurons per imaging site. Each dot is an imaging site.

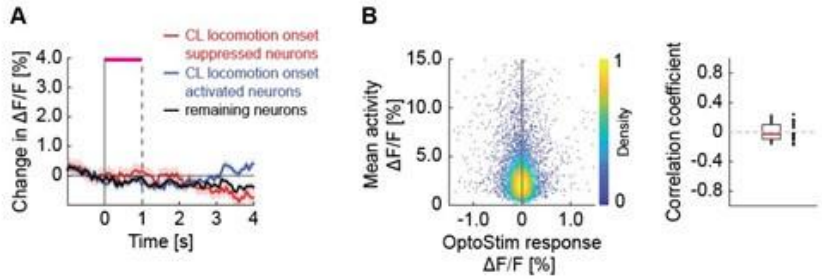

> *(Minor comments)*
>
> *1. It is unclear which BF subregion(s) were targeted in this study.*

Thanks for pointing this out. We targeted the entire basal forebrain (medial septum, vertical and horizontal limbs of the diagonal band, and nucleus basalis) with our viral injections. All our axonal imaging data comes from visual cortex and given the sensory modality-selectivity of cholinergic projections to cortex, the labeled axons originate from medial septum and the diagonal bands (Kim et al., 2016). We have now added the labels for basal forebrain subregions targeted next to the injection coordinates in the manuscript.

> *1. Page 43, Line 818: The journal name of the cited paper Collins et al. is missing.*

Fixed.

> *1. In the optogenetic experiments, how long is the inter-trial interval? Simulation of BF is known to have long-lasting effects on cortical activity and plasticity. It is, therefore, important to have a sufficient interval between trials.*

The median inter-trial interval for different stimulation events are as follows:

- Optogenetic stimulation only : 15 s
- Optogenetic stimulation + grating : 12 s
- Optogenetic stimulation + mismatch: 35 s
- Optogenetic stimulation + locomotion onset: 45 s

We have added this information to the methods in the manuscript.

Assuming locomotion is the primary driver of acetylcholine release (as we argue in Figures 1 and 2), the frequency of stimulation roughly corresponds to the frequency of acetylcholine release experienced endogenously. It is of course possible that being awake and mobile puts the entire system in a longlasting acetylcholine driven state different from what would be observed during long-term quite wakefulness or during sleep. But the main focus of the optogenetic stimulation experiments we performed was to investigate the consequences of the rapid acetylcholine release driven by locomotion.

1. *Page 11, Line 313: "..., we cannot exclude the possibility of a systemic contribution to the effects we observe through shared projections between different cortical and subcortical target." This possibility can be tested by examining the effect of optogenetic stimulation of cholinergic axons on locomotor activity, as they did for the chemogenetic experiments (Fig. S7). If the optogenetic manipulation changes locomotor activity, it is likely that this manipulation has some impact on subcortical activity and systemic contribution to the changes in cortical responses observed.*

Based on the reviewer suggestion we tested this and found no change in the locomotor activity of the mice on optogenetic stimulation of cholinergic axons locally in visual cortex (we have added this as Figure S5 to the manuscript). Please note however, we can of course not exclude a systemic contribution based on this.

1. *Fig. 4 and 5: In a closed-loop configuration, L2/3 neurons exhibit a transient increase in response at the onset of locomotion, while in an open-loop configuration, their response is more prolonged. On the other hand, L5 neurons show a sustained response in both configurations. Do the authors have any speculation on this difference?*

This is correct. Locomotion onset responses in layer 2/3 are strongly modulated by whether the locomotion onset occurs in closed loop or open loop configurations (Widmer et al., 2022). This difference is absent in our layer 5 data here. We suspect this is a function of a differential within-layer cell type bias in the different recordings. In the layer 2/3 recordings we are likely biased strongly towards superficial L2/3 neurons that tend to be negative prediction error neurons (top-down excited and bottom-up inhibited), see e.g. (O'Toole et al., 2023). A reduction of locomotion onset responses in closed loop is what one would expect for negative prediction error neurons. While layer 5 neurons exhibit mismatch responses, they do not exhibit opposing top-down and bottom-up input that would result in such a suppression (Jordan and Keller, 2020).

We can illustrate this by splitting all layer 2/3 neurons based on their response to gratings and to visuomotor mismatch into a positive prediction error (PE) type (top 30% positive grating response), a negative prediction error type (top 30% positive visuomotor mismatch response), and the rest (remaining neurons and neurons responsive to both grating and visuomotor mismatch). Plotting the response of these neurons to locomotion onset in closed loop and open loop, we find that negative PE neurons have a transient response to locomotion onset in closed loop while positive PE neurons have a sustained increase in response in closed loop. In open loop the response of the two populations is indistinguishable. Splitting the layer 5 neurons using the same criteria, we don't find a striking difference between closed and open loop between the two groups of neurons. We have added this as Figure S8.

Reviewer #2 (Recommendations For The Authors):

Major concerns:

1. *As a ubiquitous promoter was used to drive GCaMP expression, please explain how excitatory neurons were identified.*

1. *As the data cover a very small range of running speeds, it is important to confirm that the binary locomotion signal model still applies when mice run at higher speeds - either by selecting recordings where mice have a wider range of running speeds or conducting additional experiments. In addition, please show the running speed tuning of individual axons.*

> 1. *Please provide a more detailed analysis of the effects of locomotion and cholinergic modulation on visual responses. How does cholinergic modulation affect orientation and direction tuning? Are the effects multiplicative or additive? How does this compare to the effects of locomotion on single neurons?*
>
> 1. *To ensure that the analyses in Figure 5 are not confounded by differences in the visual stimulus, please include average visual flow speed traces for each condition.*
>
> 1. *Please clarify why chemogenetic manipulations of cholinergic inputs had no effect on pairwise correlations in L2/3.*
>
> 1. *The latency effect is quite an extraordinary claim and requires careful analysis. Please provide examples of single neurons illustrating the latency effect - including responses across individual grating orientations/directions. One possible confound is that grating presentation could itself trigger locomotion or other movements. In the stationary / noOpto conditions, the grating response might not be apparent in the average trace until the animal begins to move. Thus the large latency in the stationary / noOpto conditions may reflect movement-related rather than visual responses.*

Please see our responses to these points in the public review part above.

> *There are some minor points where text and figures could be improved:*
>
> 1. *When discussing the decorrelation of neuronal responses by cholinergic axon activation, it is important to make it clear that Figure 6D quantifies the responses of layer 5 apical dendrites rather than neurons.*

We have added this information to the results section.

> 1. *In Figure S7, please clarify why velocity is in arbitrary units.*

This was an oversight and has been fixed.

> 1. *Please clarify how locomotion and stational trials are selected in Figure 4.*

We thank the reviewers for pointing this out. Trials were classified as occurring during locomotion or while mice were stationary as follows. We used a time-window of -0.5 s to +1 s around stimulus onset. If mice exhibited uninterrupted locomotion above a threshold of 0.25 cm/s in this time-window, we considered the stimulus as occurring during locomotion, otherwise it was defined as occurring while the mice were stationary. Note, the same criteria to define locomotion state was used to isolate visuomotor mismatch events, and also during control optogenetic stimulation experiments. We have added this information to the methods.

> 1. *When testing whether cholinergic activation is sufficient to explain locomotion-induced decorrelation in Figure 6G-H, please show pre-CNO and post-CNO delta-correlation, not just their difference.*

We can do that, but the results are harder to parse this way. We have added this as Figure S11 to the manuscript. The problem with parsing the figure is that the pre-CNO levels are different in different groups. This is likely a function of mouse-to-mouse variability and

makes it harder to identify what the CNO induced changes are. Using the pre-post difference removes the batch influence. Hence, we have left this as the main analysis in Figure 6G and 6H.